

Philippe Oberhemm BSc of Engineering

Characterization of a carboxylic acid reductase from
Neurospora crassa

Masterarbeit

zur Erlangung des akademischen Grades
Master of Engineering- Biotechnology

Eingereicht an der
Technischen Universität Graz

Betreuer/in

Herr Assoc. Prof. Dipl.-Ing. Dr.techn. Harald Pichler

Frau Dipl.-Ing. Dr.techn. Margit Winkler

Graz, Oktober 2017

EIDESSTATTLICHE ERKLÄRUNG

Ich erkläre an Eides statt, dass ich die vorliegende Arbeit selbstständig verfasst, andere als die angegebenen Quellen/Hilfsmittel nicht benutzt und die benutzten Quellen wörtlich und inhaltlich entnommenen Stellen als solche kenntlich gemacht habe. Das in TUGRAZonline hochgeladene Textdokument ist mit der vorliegenden Masterarbeit identisch.

Datum Unterschrift

Danksagung

Die vorliegende Studie wurde an der Technischen Universität Graz unter der Betreuung von Frau Dr. Winkler durchgeführt.

An erster Stelle möchte ich Herrn Prof. Dr. Pichler für die Betreuung meiner Masterarbeit danken. Weiterer Dank gilt Frau Dr. Winkler, welche mir im Rahmen Ihrer Studien die Mitarbeit am Projekt ermöglichte und mich dabei fachlich unterstützte. Des Weiteren Herrn Schwedenwein, der immer ein offenes Ohr hatte und mir darüber hinaus, mit Rat und Tat zur Seite stand. Ein weiterer Dank geht an meine Kommilitonin Frau Hirschböck, welche sich mit mir ein Büro teilte und dabei bei verschiedenen Fragen zur Seite stand. Außerdem Herrn Dr. Strohmeier für die Möglichkeit der GC-FID-Messungen im Rahmen dieser Studie, sowie die fachliche Beratung.

Last but not least möchte ich einen besonderen Dank an meine Eltern richten, welche mich während des Studiums in jeder Lebenslage unterstützt haben

Besonderer Dank gilt auch dem Squash-Team UWK Kardamint, das mich seit meiner Ankunft in Graz aufgenommen und österreichischen Sitten entsprechend sozialisiert hat.

Kurzzusammenfassung

Diese Masterarbeit behandelt die Charakterisierung einer Karbonsäurereduktase. Die Gensequenz wurde aus dem Pilz *Neurospora crassa* isoliert und das entsprechende Enzym (*NcCAR*) in *E.coli* exprimiert. Zum ersten Mal beschrieb Gross dieses Enzym in den 1960ern. In den weiteren Publikationen wurde diese Enzymklasse näher erforscht; und diese offeriert letztendlich eine Möglichkeit zum Einsatz in der Weißen Biotechnologie zur Gewinnung von Aldehyden. Dabei können die *in vitro* gewonnenen Erkenntnisse später für Zellumsetzungen *in vivo* als Referenzdaten genutzt werden. Aldehyde finden Anwendung in der Lebensmittelindustrie oder werden als Duftstoffe eingesetzt. Der Großteil dieser Aldehyde wird zurzeit noch durch die chemische Aldehyde-Synthese gewonnen.

In dieser Abhandlung wurde *NcCAR* in *Escherichia coli* BL21 (DE3) mittels Autoinduktion bei einer Temperatur von 28°C exprimiert. Im Anschluss an die Kultivierung wurde die Zellmasse geerntet und mittels Ultraschallbehandlung aufgeschlossen. Das daraus gelöste Enzym, wurde mittels His-Tag, optionaler Abspaltung des His-Tags, sowie eines weiteren Gelfiltrationsschrittes aufgereinigt. Die gewonnenen *NcCAR*-Präparationen dienten im Anschluss der Charakterisierung. Dabei wurde ein indirekter fotometrischer Assay mit Hilfe eines Plattenlesers, basierend auf dem Verbrauch von NADPH, verwendet. Zur Verifizierung der gewonnenen Resultate wurden im weiteren Verlauf HPLC- und GC-Messungen durchgeführt. Dabei wurden die optimalen pH-Bedingungen, Pufferzusammensetzung, Temperatur, sowie verschiedene Substrate untersucht. Hierbei zeigte sich die höchste Enzymaktivität unter Verwendung eines MES-Puffers, pH 5,5, mit 10 mM MgCl₂, gemessen bei einer Temperatur von 35°C. Des Weiteren zeigte sich, dass *NcCAR* eine umfassende Substratazeptanz von aliphatischen und aromatischen Säuren aufwies. Die höchste Aktivität wurde bei der Verwendung von α -Methyl-Zimtsäure als Substrat beobachtet. Zusätzlich wurde die Temperaturstabilität der *NcCAR* untersucht. Darüber hinaus wiesen Veröffentlichungen auf einen inhibierenden Effekt des Co-Produkts Pyrophosphat auf die Aldehydproduktion hin, welche im Verlauf dieser Arbeit untersucht wurde. Abschließend wurden die kinetischen Parameter v_{\max} 16,59 mM/min und K_M 1,732 mM mit Zimtsäure als Substrat, basierend auf dem Michaelis-Menten Modell, berechnet. Diese Enzymcharakterisierung vergleicht die bereits gewonnen und publizierten Daten und soll diese im Zuge der Analyse erweitern.

Abstract

This master thesis is focused on the characterization of a fungal carboxylic acid reductase. Its gene sequence was isolated from *Neurospora crassa* and the protein (*NcCAR*) was expressed in *Escherichia coli*. The corresponding enzyme was first published in the 1960s by Gross. This specific enzyme offers an alternative possibility to generate aldehydes in the field of white biotechnology. The enzymatic process offers an alternative to the chemical aldehyde production. Alternatively, those aldehydes can be used as fragrances or as flavours. CARs can be used in vivo or without cellular systems. In this thesis, *NcCAR* was cultivated in *E. coli* BL21 (DE3) using an autoinduction protocol. The enzyme expression was performed at 28 °C. After the cultivation process, the cells were centrifuged and sonicated for downstream processing (Ni-affinity chromatography purification, optional cleavage of the His-Tag, or gel filtration). The enzyme was characterized by indirect photometric NADPH depletion assays. Some biotransformation reactions were additionally analysed by HPLC and GC. The optimal reaction conditions with respect to pH, buffer composition, temperature and co-solvent tolerance for the aldehyde generation were investigated. The conditions for the highest enzyme activity were determined to be MES buffer, pH 5.5, with 10 mM MgCl₂ at 35°C. *NcCAR* revealed a broad substrate range of aliphatic and aromatic acids. The highest activity was observed with α -methyl-cinnamic acid. In addition, the temperature stability of the *NcCAR* was determined. Based on published literature, the inhibition of the reaction by the co-product pyrophosphate was analysed and was reduced by addition of pyrophosphatase. Finally, the kinetic parameters of $v_{\max} = 16,59$ mM/ min and $K_M = 1,732$ mM with cinnamic acid as substrate were calculated on the basis of the Michaelis-Menten model. These values were compared to published data and expand the knowledge of the carboxylic acid reductase of *Neurospora crassa* during this thesis.

1 Table of Content

Kurzzusammenfassung

Abstract

1	Table of Content	
2	Introduction	
3	Materials and Methods	
3.1	Vector system for expression of the <i>Ni</i> CAR without PPTase	7
3.2	Vector system for co-expression of <i>Nc</i> CAR and <i>Ec</i> PPTase in <i>E. coli</i>	7
3.3	Autoinduction procedure for protein expression in <i>E. coli</i>	7
3.4	His-Tag purification of the <i>Nc</i> CAR	8
3.5	Manual purification of the <i>Ni</i> CAR (<i>Nocardia sp.</i> -CAR) protein	9
3.6	Fermentation and purification procedure of the phosphopantetheinyl-transferase (pMS470- <i>Gk</i> PPTase in <i>E. coli</i> BL21 (PPTase))	10
3.7	SDS-PAGE to control the purification procedure	11
3.8	<i>Nc</i> CAR activity assays with Synergy MX-Plate reader	11
	<i>Nc</i> CAR cosolvent tolerance	12
	<i>Nc</i> CAR buffer screening	13
	<i>Nc</i> CAR temperature optimum	13
	<i>Nc</i> CAR temperature stability	14
	Kinetic parameters of <i>Nc</i> CAR with cinnamic acid	14
3.9	HPLC (High Performance Liquid Chromatography) analysis	15
3.10	GC-MS (Gas chromatography-Mass spectroscopy) analysis	15
3.11	Fermentation and purification procedure of <i>Gk</i> PPTase	16
3.12	Pyrophosphatase (PPase) assay	16
3.13	Influence of additional phosphopantetheinylation on the enzymatic activity of recombinant CARs	17
4	Results	
4.1	Expression and purification of <i>Nc</i> CAR	18

Table of content

4.2	Results of the <i>Ni</i> CAR purification.....	25
4.3	Results of the PPTase purification.....	26
4.4	Results of the substrate screening with <i>Nc</i> CAR.....	27
4.5	Verification of aldehyde production by GC-FID	28
4.6	The optimal pH conditions for <i>Nc</i> CAR.....	32
4.7	Optimal temperature for <i>Nc</i> CAR mediated carboxylate reduction	34
4.8	Temperature stability of the enzyme	35
4.9	Results of the enzyme kinetics.	36
4.10	Phosphopantetheine transferase assay	37
4.11	Influence of pyrophosphate	38
5	Discussion	
6	Appendix	
6.1.1	Centrifuges and associated materials	49
6.1.2	Fast protein liquid chromatography (FPLC) and materials.....	49
6.1.3	SDS-PAGE and materials	49
6.1.4	HPLC and associated materials.....	49
6.1.5	GC-FID.....	50
6.1.6	Columns	50
6.1.7	Photometer and associated materials.....	50
6.1.8	Reaction vessels	51
6.1.9	Shakers and incubators.....	51
6.1.10	Additional instruments and materials.....	51
6.2	Reagents, buffers, stocks and media.....	51
6.3	Received organisms	52
6.4	Software.....	52

2 Introduction

This master thesis is focused on the characterization of a carboxylic acid reductase encoded by a gene sequence from the fungus *Neurospora crassa* (*NcCAR*, NCBI accession code XP_955820.1). The gene sequence of the carboxylic acid reductase from *N. crassa* was delivered by Margit Winkler. She compared the known sequences from literature (*NiCAR* Q6RKB1.1, *MmCAR* B2HN69, *SrCAR*, WP_013138593.1 and *AtCAR* XP_001212808.1) by blastp search against the Gen-Bank¹ non-redundant protein sequence of *N. crassa* (taxid:5241). The final output showed low sequence identity to the initial protein sequences *NiCAR*, *MmCAR*, *SrCAR* and *AtCAR* (17.3%, 17.5%, 18.5% and 22.5%, respectively),¹ as well as low conformity to the published CARs. The vector used for expression of *NcCAR* is called pET-Duet1_*EcPPTaseHTNcCAR* and was used for the functional protein expression in *E. coli* BL21 (DE3) gold **Figure 1**.² The vector construct is designed to simultaneously express two proteins. A phosphopantetheine transferase (PPTase), required for the activation of the *NcCAR*, and the *NcCAR* itself. The gene sequence of *NcCAR* was optimized for the *E. coli* codon usage and extended with the gene of the PPTase of *E. coli* (NCBI gene accession Nr. CAQ31055.1). The vector construct may protect individual subunits from degradation. The capability of the Duet vectors for protein co-expression makes them ideal for the production of protein complexes.¹ *E. coli* BL21 contains in its genome the T7 polymerase under control of the lac operator. The expression of those genes is induced by a *lac*-operon, which contains the T7 promoter region. Further, a 6xHis-Tag attached to the N-terminal side of the *NcCAR* sequence for simplified purification was added. A TEV cleavage site was arranged between the coding sequences for the His-Tag and the *NcCAR*. The *NcCAR* gene sequence is arranged between the restriction sites *NdeI* and *XhoI*. The pET-Duet1_*EcPPTaseHTNcCAR* contains an ampicillin resistance gene. In total, the plasmid contains 9158 bp. The expressed PPTase of *E. coli* is used to activate *NcCAR*.

¹ pETDuet%E2%84%A2-1-DNA---Novagen,EMD_BIO-71146 @ www.merckmillipore.com 06.2017

Introduction

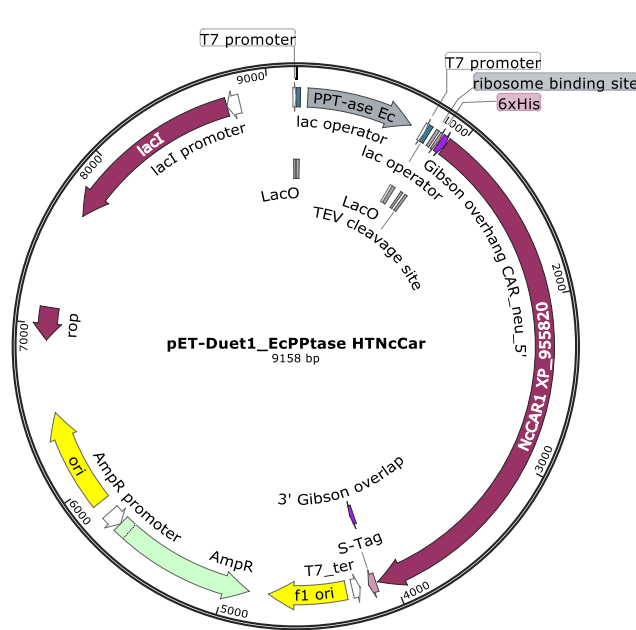


Figure 1: The pet-Duet1_EcPPTaseHTNcCAR vector was constructed by Margit Winkler ².

NcCAR was first described by Gross and Zenk in 1968,⁴ who isolated the protein from its natural host. The literature gives no information about their used protein sequence. One of the aims of this thesis was to compare the characteristics of recombinant *NcCAR* with those of *CAR* isolated from *N. crassa*. They isolated and partially purified two enzymes from mycelia of *N. crassa* (Wild-type, SY7A, Fungal Genetic Stock Center Nr. 622)⁵ which catalyses the reduction of aromatic acids to aromatic aldehydes, as well as the reversible reduction of aromatic aldehydes to aromatic alcohols.⁴ The first enzyme had its pH optimum at 8.0, temperature optimum at 35°C, and was stable for at least two months, if kept at 0°C in presence of dithiothreitol. The molecular weight was estimated around 120 kDa. Gross also analysed the enzyme substrate intermediates in the aryl-aldehyde NADP oxidoreductase reduction of salicylate. In the described reaction of the transfer of hydrogen from NADPH to the acid, ATP was shown to be split into AMP and pyrophosphate. This fact demonstrated that ATP served as the energy donator in this endergonic process. With the analysed conditions they failed to demonstrate the formation of salicylic aldehyde from enzyme-AMP in the presence of salicylate and NADPH.⁶

In general, carboxylic acid reductases such as the analysed *NcCAR* can reduce carboxylic acids to their corresponding aldehydes. The generated aldehydes are useful in industrial applications, such as flavours and fragrances.^{7, 8, 9, 10} For example, benzaldehyde and vanillin are two

Introduction

aromatic aldehydes and are most widely used as flavouring agents.¹¹ Carboxylic acid substrates are available in great abundance from renewable sources e.g. vanillic acid, ferulic acid and many others.¹² Right now, those flavours and fragrances are mainly produced by chemical synthesis, but the industry is met with the problem, that carboxylic acid reductions demands strong reduction power.¹² To challenge the industrial production with an enzymatic pathway, an efficient reductive process will become necessary. The reduction is a challenge for chemical conversions as well as for enzymatic reactions in metabolic pathways.¹³ The difficulty is based on the chemical structure of the carboxylic acid moiety. The -COOH group is in an energetically favoured state, due to its highest oxidation state and needs an uncommon energy activation to participate in chemical reactions. When the energetic barrier is overcome, the reactive aldehyde can be produced. Further reduction of the aldehyde to the primary alcohol may happen, as illustrated in Figure 2.¹² In comparison, the chemical synthesis of aldehydes is often performed by lithium tri-*t*-butoxy aluminium hydride¹⁴ or DIBALH¹⁵ as catalyst. Currently, the chemical strategy is the over-reduction to the alcohol and the further re-oxidation to the corresponding aldehyde by e.g. Swern oxidation.¹⁶ Those procedures are either expensive or use environmentally harmful reagents.

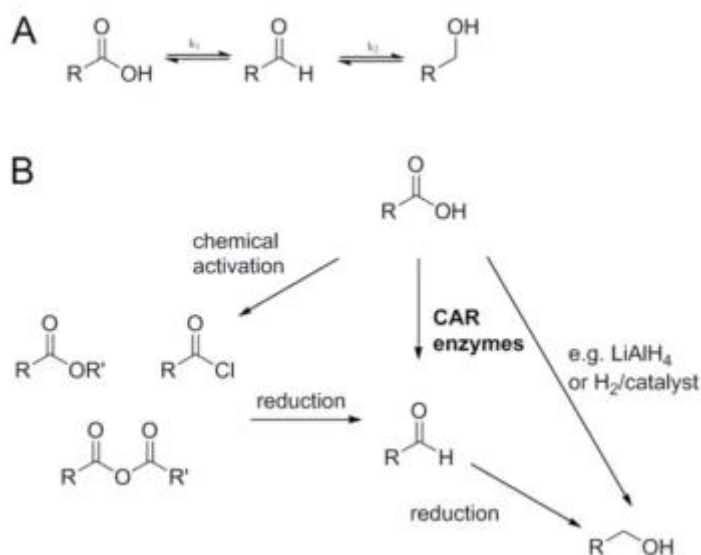


Figure 2 (A) Reduction of carboxylic acids ($k_1 \ll k_2$), k_1 and k_2 – reaction rate coefficients for the reduction of carboxylic acid to aldehyde (k_1) and aldehyde to alcohol (k_2). (B) A simplified overview of strategies for the reduction of carboxylic acids. The two most often applied routes of carboxylic acid reduction versus the biocatalytic route.¹²

Introduction

CARs are ~ 120 kDa multidomain enzymes. The basic construction of the *Nc*CAR contains three domains as illustrated in **Figure 3**. An adenylyating domain (A-domain), a phosphopantetheinyl binding domain and a reduction domain (R-domain). For the enzyme activation, a phosphopantetheine arm must be covalently attached to the serine residue, in the centre domain of the enzyme. The procedure is catalysed by a phosphopantetheine transferase (PPTase). PPTase uses Coenzyme A (CoA) and ATP which gets dephosphorylated to ADP during the activation process. Without phosphopantetheinylation the enzyme is called apo-CAR. Upon phosphopantetheinylation a holo-CAR (EC 1.2.1.30) is formed.¹⁷

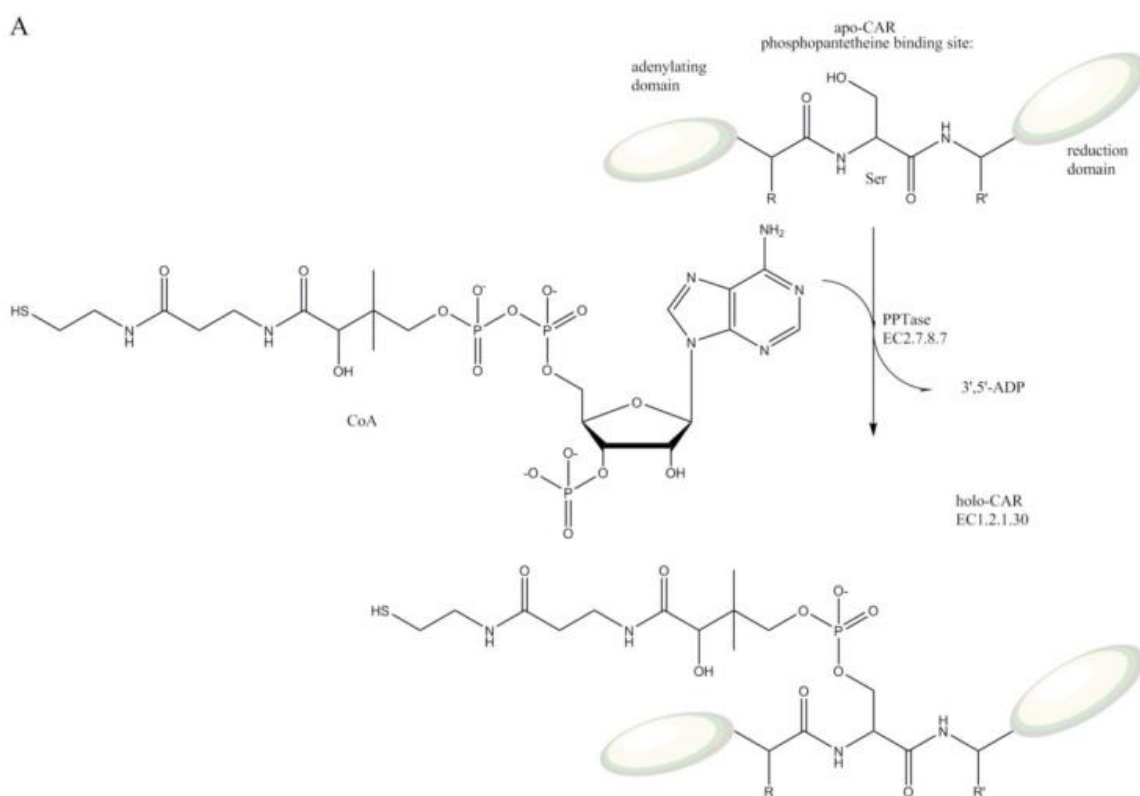
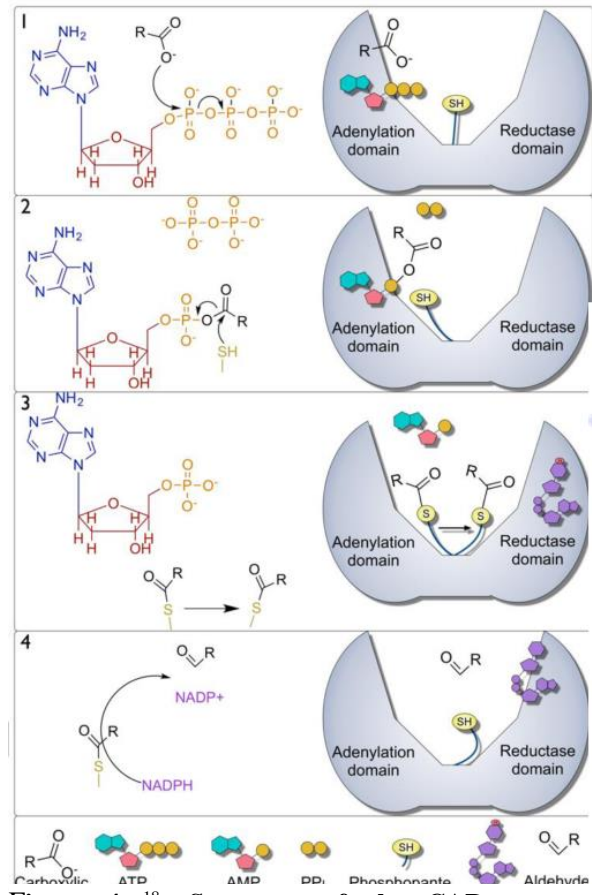


Figure 3. Post-translational modification of carboxylate reductases. The phosphopantetheine moiety gets attached to the CoA as donor and binds to the conserved serine residue of the apo-CAR. The whole reaction is catalyzed by PPTase. One PPT-binding site motif is e.g. LGG-x-S-xx-A.¹²

Introduction

The enzyme mechanism can be divided into four steps as illustrated in **Figure 4**.¹⁸ The first (1) step occurs in the adenylating domain of the CAR. The relatively unreactive carboxylic acid is activated by forming a thioester with the phosphopantetheine arm. The cofactor ATP and the carboxylic acid enter the A-domain. There, oxygen of the carboxylic acid attacks the α -phosphate of ATP forming an AMP-acyl phosphor ester. The remaining pyrophosphate is released and acts like an inhibitor for the mechanism.^{19, 20} Then (2), a nucleophilic attack occurs onto the carbonyl carbon of the AMP-acyl phosphor ester intermediate, by the phosphopantetheine arm. AMP is released and an acyl thioester with the phosphopantetheine arm is formed. The generated acyl thioester is then transferred to the C-terminal reductase domain, managed by the phosphopantetheine arm (3). In the C-terminal reductase domain the thioester is reduced by NADPH to the final aldehyde. The NADP^+ and the aldehyde is released regenerating the thiol of the phosphopantetheine arm for further reactions (4).¹²



Introduction

The cell-free-conversion can be used further, to develop a cell-based microbial conversion.^{21, 22} The advantage of using a whole-cell biotransformation is based on the possibility of cofactor regeneration, but it can create problems for the host cells, because of toxicity of the aldehyde. In contrast, cell-free conversions circumvent the over reduction of the aldehyde, but the addition of cofactors is needed.²² The whole cell conversion will not be a part of this thesis.

The final goal of this thesis was a comprehensive characterisation of *NcCAR* including determination of the temperature, pH/buffer, co-solvents optima as well as a broad substrate screening with aliphatic and aromatic acids. The data generated in this thesis will be compared with the already existing data of Gross as well as with carboxylic reductases like *MpCAR*, *NiCAR*, *NoCAR*, *TpCAR*¹⁸ and the carboxylic reductase of *Nocardia sp.*^{7,24}.

3 Materials and Methods

3.1 Vector system for expression of the NiCAR without PPTase

The vector pEHISTEV_NiCAR_opt in *Escherichia coli-BL21 gold (E. coli)* was received as a glycerol stock from Margit Winkler.

3.2 Vector system for co-expression of NcCAR and EcPPTase in E. coli

The pET-Duet1_EcPPTaseHTNcCAR vector² was used for the expression of holo-NcCAR in *E. coli* BL21 (DE3) gold and was delivered by Margit Winkler (Figure 1).

3.3 Autoinduction procedure for protein expression in E. coli

100 ml of the preculture medium was inoculated with 5 µl of a glycerol stock and was incubated at 37°C and 295 rpm overnight in baffled Pyrex 250 ml Narrow Mouth Erlenmeyer Flasks. The media contained the components shown in Table 1.

Table 1. Overview of preculture media components

Preculture medium	Concentration
MgSO ₄	1 mM
Glucose	4.4 mM
Ammonium sulphate	2.5 mM
Potassium dihydrogen phosphate	5 mM
Ampicillin	50 mg/l
Total volume	100 ml

Material and Methodes

0.8 ml of this overnight preculture was used to inoculate 400 ml of the main culture in baffled PYREX 1 L Narrow Mouth Erlenmeyer Flasks which contained the components shown in Table 2.

Table 2 Overview of the main culture components for shake flask fermentation

Main culture medium	Concentration
Magnesium sulphate	1 mM
Glycerol	54 mM
Glucose	2.8 mM
α -Lactose	5.8 mM
Ammonium sulphate	25 mM
Potassium dihydrogen phosphate	50 mM
Ampicillin	50 mg/L
Total volume	1 L

The incubation was carried out in two steps. The first step was performed for 4 h at 37°C and 180 rpm. Subsequently, the second step of the cultivation was carried out between 140 and 160 rpm at 20°C for 20 h to express the proteins. After 24 h, the cells were harvested and centrifuged at 4000 rpm for 10 min at 4°C using the Avanti™ centrifuge J-20 XP/Beckman Coulter™ centrifuges with a JA 10 rotor mentioned in the appendix (7.1.1). The shakers shown in 7.1.9 were used for the cultivation. The supernatant was discarded and the cell pellet was resuspended in ~25 ml CAR-storage buffer Table 12 for the sonication process. The sonication (Sonopuls HD2070) was performed in two steps of 3 min with a pulse of 80 %.

3.4 His-Tag purification of the *NcCAR*

The protein was purified by Nickel-affinity chromatography using the ÄKTA purifier 100. The elution samples were collected with a fraction collector Frac-950. Therefore, the frozen cells from the cultivation procedure, as mentioned in 3.3, were suspended in buffer-A with the buffer composition mentioned in 7.2. The cells were disrupted using ultra-sonication with two cycles of 3 min by a pulse of 80 %. The sample was centrifuged using an ultracentrifuge Optima LE80K with the rotor Type 70 Ti at 40,000 rpm mentioned in 7.1.1 for 45 min and 4°C. The supernatant of the centrifugation containing buffer-A was loaded onto the His Trap™ FF column (5 ml). After that, a washing step with ~5 CVs (column volume) was performed, until the UV-baseline was reached with buffer-A. The flow-through was collected and the elution was started with buffer-B (described in 7.2). For the first purification batch, a gradient was performed by increasing the buffer-B concentration from 0 % up to 100 % over a time of

Material and Methodes

10 CVs. After the elution point was known, an isocratic run containing three steps with 10 %, 25 % and 100 % buffer-B were performed for further purification batches. The enzyme containing samples were pooled and the buffer was changed to CAR-Storage buffer, via using the ÄKTA prime system with a HiPrep™ 26/10 desalting column. 10 % (v/v) of glycerol was added to the samples. After the buffer exchange, the protein samples were concentrated to ~10 mg/ml by the use of Vivaspin columns with a 30 kDa cut-off and aliquots of 500 µl were stored at -80°C.

To increase the purity of the enzyme the TEV-cleavage side was used to remove the His-Tag of the enzyme. The sample was incubated with TEV-protease at a ratio of 1:10 to the *NcCAR* and was incubated over night at 4°C. The sample was loaded with buffer-A onto a His Trap™ FF column (5 ml). After that, buffer-A was exchanged by CAR-storage buffer, using the PD-10 Desalting Column GE Healthcare Life Sciences protocol. The flow-through, containing the *NcCAR*, was collected and concentrated with Vivaspin 20 centrifugal concentrators. Aliquots of 500 µl were stored at -80°C.

Alternatively, a sample of *NcCAR* was purified by using a gel-filtration HiLoad™ 16/60 Superdex™ 200 prep column. 6 mg/ml His-Tag™ purified enzyme was loaded onto the column. The run was performed with CAR-Storage buffer with a flow-rate of 3 ml/min and the flow-through was collected. The detailed materials are described in the appendices 7.1.2 and 7.1.6.

3.5 Manual purification of the *NiCAR* (*Nocardia* sp. -CAR) protein

The designed strain of *NiCAR* of *Nocardia* sp. did not contain a phosphopantetheine transferase (PPTase), required for the activation of the enzyme. PPTase was added after the purification of *NiCAR* to generate the final holo-*NiCAR*. The holo-*NiCAR* was used to compare the activation of the *NcCAR* as a positive control as well as to analyse the ability for additional post-clonal activations with additional PPTase. A cell pellet containing recombinant holo-*NiCAR* was delivered by Margit Winkler.

The protein was purified by Nickel-affinity chromatography. The elution samples were collected in 15 ml tubes. Therefore, the delivered frozen cells were suspended in buffer-A with the buffer composition mentioned in 7.2. The cells were disrupted using ultra-sonication with two cycles of 3 min by a pulse of 80 %. The sample was centrifuged using an Optima LE80K at 40,000 rpm with the rotor type 70 Ti mentioned in 7.1.1 for 45 min and 4°C. The supernatant

Material and Methodes

of the centrifugation containing buffer-A was loaded on to the His TrapTM FF column (5 ml) manually with a syringe. After that, a washing step with ~10 CVs was performed. The flow-through was collected and the elution was started with buffer-B (described in 7.2). The elution was performed with additional buffers containing 25, 50, 62.5, 75, 87.5, 93.75, and 100 mM imidazole, 500 mM sodium chloride and 20 mM potassium dihydrogen phosphate. To control the protein concentrations of the different fractions, a BCA assay was applied. BSA in a concentration range between 0 and 2000 µg/ml was used as a standard. The protein containing fractions were pooled. After that, the buffer was exchanged by CAR-storage buffer, using the PD-10 Desalting Column GE Healthcare Life Sciences protocol, and samples were analysed by SDS-PAGE. After the buffer exchange, the protein samples were concentrated to ~10 mg/ml by the use of Vivaspin columns with a 30 kDa cut-off and aliquots of 500 µl containing 10 % (v/v) of glycerol were stored at -80°C.

3.6 Fermentation and purification procedure of the phosphopantetheinyl-transferase (pMS470-GkPPTase in *E. coli* BL21 (PPTase))

The gene sequence of *NcCAR* was optimized for *E. coli* codon usage. The designed vector includes the PPTase gene of *E. coli* (NCBI gene accession Nr. CAQ31055.1). The gene sequences were provided by Margit Winkler and had been cloned into *E. coli* by Daniel Schwendenwein. As mentioned, the phosphopantetheine-transferase is needed to activate the enzyme by a posttranslational modification. The PPTase is covalently attached to a phosphopantetheinyl from Co-enzyme A (CoA) as described in the introduction. During this study, a thermophilic PPTase of *Geobacillus kaustophilus* was chosen as an alternative PPTase to the one of *E. coli*. Because the *G. kaustophilus* PPTase is thermostable, the purification procedure becomes simple by using a heat precipitation protocol.²⁹ 25 ml preculture with 0.1 % MgSO₄, 2 ml of 40 % glucose and 5 ml 20*NPS with kanamycin as antibiotic was prepared. The main culture of 400 ml contained, in addition, 0.2 % of 50*5052 media and no additional glucose. 800 µl of the preculture with an OD₆₀₀ of 6.02 were used to incubate 400 ml main culture.

To check for the integrity of the plasmid, 1 ml of the preculture was centrifuged for 6 min at 5000 rpm in a table top centrifuge for minipreparation. The plasmid preparation was incubated with *Hind*III and *Eco*RI restriction enzymes and was loaded onto a 1 % agarose gel. The expression of the *GkPPTase* gene from the pMS470-*GkPPTase* vector in *E. coli* BL21 with ampicillin resistance was done, by inducing the main culture with 0.2 mM IPTG for 21 h

Material and Methodes

between 140 and 160 rpm and 28°C. The main culture was centrifuged for 4 min at 10,000 rpm with a J-20 XP/Beckman Coulter™ JA-10 rotor and 4°C. The final cell pellet weighed 3.2 g. The cell pellet was dissolved in CAR-Storage buffer and sonicated two times for 3 min by pulse of 80 % to disrupt the cells. The disrupted cell solution was centrifuged for 4 min at 10,000 rpm with a J-20 XP/Beckman Coulter™ JA-10 rotor and 4°C. After that the supernatant was treated for 10 min at 70°C and was finally centrifuged for 10 min by 4000 rpm with a J-20 XP/Beckman Coulter™ JA-10 rotor and 4 °C. To control enzyme expression and the thermostability of *GkPPTase*, an SDS-PAGE was performed (see next section).

3.7 SDS-PAGE to control the purification procedure

4 µl NuPAGE LDS Sample Buffer (4X) was added to 10 µl of protein samples. The samples were heated at 85°C for 10 min. Subsequently, the samples were loaded onto a NuPAGE® Bis-Tris gel as described in 7.1.3. Five µl of the PAGE Ruler Prestained Protein Ladder 10-180 kDa was used as standard. The run was performed with constant voltage of 200 V and a runtime of 50 min with MOPS-buffer. The proteins were visualized by treating the gel for 1 h with Simply Blue solution. Subsequently, the gel was treated with ddH₂O to enhance the colour differences between the protein and the gel overnight.

3.8 *NcCAR* activity assays with Synergy MX-Plate reader

All experiments were carried out with a minimum of biological duplicates and technical quadruplicates in UV-Star 96 well plates as well as blank reactions without the enzyme preparation. Additional CAR-Storage buffer was added instead. A Synergy MX-plate reader (see 7.1.7) was used to analyse the depletion of NADPH caused by the *NcCAR* mediated carboxylate reduction over a time of 10 min at 28°C and a wavelength of 340 nm if not mentioned otherwise. The used photometer protocol started with a mixing step of 30 s. In general, the measurement was performed in a total volume of 200 µl. The assay composition is shown in Table 3. The potential carboxylic acid substrates were dissolved in DMSO or KOH at a stock concentration of 100 mM and a final concentration of 5 mM for the screening procedure. The reaction was started by adding NADPH and ATP (0.5 mM and 1 mM) final concentration, respectively. Blank reactions without the enzyme preparation were performed in parallel. The missing 10 µl of the enzyme preparations were replaced with 10 µl of CAR-Storage buffer.

Table 3: Overview of the components included to determine the enzyme activity of *NcCAR*.

	Final concentration	Unit	Components
Buffer	80	mM	100 mM TrisHCl, pH 7.5; 10 mM MgCl ₂ ²
Substrate	5	mM	Dissolved in DMSO
Enzyme	~0.05	mg/mL	<i>NcCAR</i> in CAR-Storage buffer
NAD(P)H	0.5	mM	Dissolved in ddH ₂ O
ATP	1	mM	Dissolved in ddH ₂ O
Methanol	0 - 40	% v/v	Dissolved in ddH ₂ O
DMSO	0 - 40	% v/v	Dissolved in ddH ₂ O

NcCAR cosolvent tolerance

Every chosen and screened substrate was dissolved in DMSO or 0.1 M KOH. Due to the possible influence of DMSO as solvent on the enzyme activity, a dilution series was made. The concentrations of DMSO or methanol as reference constituted 0.8 %, 1.6 %, 4 %, 8 %, 12 %, 16 %, 24 %, and 40 %. As final concentration 5 mM cinnamic acid substrate, 0.5 mM NADPH and 1 mM ATP were used. About 0.027 mg/ml of *NcCAR* with one step purification preparation was used.

² Except for the pH-optimum experiments

NcCAR buffer screening

To determine the optimal pH to convert acids to aldehydes, four different buffer systems in the pH range between pH 4 and pH 10 were tested. Buffer systems are only able to operate in a specific range, based on the buffer components. Due to that fact, all buffer compositions were based on the calculation of the bioinformatics.org webpage.³ The calculated composition results of the buffer systems are shown in Table 4 with pH steps of 0.5.

Table 4. Different buffer solutions with 10 mM MgCl₂ to determine NcCAR activity in the range of pH 4 to 10

Buffer composition	Concentration [mM]	pH Ranges
Sodium citrate	100	pH 4 - pH 5.5 in 0.5 steps
MES 2-(N-morpholino)ethanesulfonic acid	100	pH 5.5 - pH 6 in 0.5 steps
Tris(hydroxymethyl)aminomethane	100	pH 7 - pH 7.5 in 0.5 steps
Glycine	100	pH 9 - pH 10 in 0.5 steps

Cinnamic acid was chosen as substrate at a final concentration of 5 mM, for all experiments. During this assay, the NADPH and ATP final concentration was 0.5 mM and 1 mM ATP, respectively.

NcCAR temperature optimum

To determine the temperature optimum of NcCAR mediated acid reduction, the temperature range between 20°C to 65°C was analysed in 5°C increments based on the plate reader assay mentioned in 3.8. Therein, the plate reader was limited as it is not able to cool or to heat up over 65°C. The chosen buffer was a 0.1 mM MES buffer with 10 mM MgCl₂. As substrate, 5 mM cinnamic acid was chosen. The final concentration of the cofactors was 0.5 mM NADPH and 1 mM ATP. As pH values decrease at increased temperature by acid dissociation, the pH values at room temperature had to be changed. The MES buffer was prepared at room temperature with corrected pH as shown in Table 5 based on the calculations of the bioinformatics.org webpage.²⁵ For the pH adjustment, 1 M NaOH was used.

³ <http://www.bioinformatics.org/JaMBW/5/4/index.html> 08.2017

Table 5. Buffer preparation and adjusted pH value for the chosen temperature profiles

Buffer composition	To be used at Temperature	corrected pH-value
100 mM MES (2-(<i>N</i>-morpholino)ethanesulfonic acid) 10 mM MgCl₂	20 °C - 30 °C	6.00
	35 °C - 40 °C	6.16
	45 °C - 50 °C	6.27
	55 °C - 60 °C	6.38

NcCAR temperature stability

The temperature stability of the enzyme was assayed by incubating a purified *NcCAR* preparation for 1.5 h at different temperatures between 0°C and 60°C in 10°C increments. Ten µl of the enzyme solution was mixed with 0.1 M Tris-HCl buffer and incubated on a thermocycler (see 7.1.9) with 350 rpm. After the incubation time of 1.5 h, 5 mM cinnamic acid, 0.5 mM NADPH and 1 mM ATP as final concentrations were added. With these compounds the reaction was started and was analysed by the Synergy MX-plate reader (see 7.1.7).

Kinetic parameters of *NcCAR* with cinnamic acid

The Synergy MX-plate reader was used to determine the maximal velocity (v_{\max}) and the Michaelis constant (K_M). Different cinnamic acid concentrations in the range between 12.8 mM to 0.00625 mM, as final sample concentrations were prepared. The generated data sets were loaded into the Sigma Plot 11.0 program to calculate the non-linear regression. All analysis was performed in technical triplicates and calculated with Sigma Plot 11.0 program with simple line & scatter error bars. The final enzyme activity was calculated by using the linear part of the NADP(H) consumption, with an extinction coefficient (ϵ) of 6.2 ml/µmol*cm measured over a time of 10 min with the plate reader. The plate thickness adds up to 0.45 cm. The calculation depends on the amount of protein used (mg/ml), which was determined by NanoDrop. The final amount of protein was calculated by the measured enzyme concentration multiplied with the volume of the protein sample (10 µl) and divided by the dilution. The total volume of the measured sample usually was 0.2 ml.

$$\text{Specific activity [U/mg]} = \frac{(\text{Total volume [ml]} * \frac{\text{Abs}}{\text{min}})}{(\text{Amount of protein [mg]} * \epsilon * \text{Thickness[cm]})}$$

Total volume [ml] = Sample volume

Abs/ min = Detected absorption over time [min]

Amount of protein = Total protein

ϵ = extinction coefficient ($6.2 \frac{\text{ml}}{\mu\text{mol} * \text{cm}}$)

Thickness = Plate coat thickness (0.45 cm)

3.9 HPLC (High Performance Liquid Chromatography) analysis

Analysis was performed by HPLC (1200 series, Agilent Technologies) equipped with a MSD SL detector using electrospray ionization, or by HPLC (1200 series, Agilent Technologies) and flame ionization detection. For the separation of the substances a Phenomenex Kinetex Biphenyl, 2.6 μ ; 100 Å; 150 x 2.1 mm column was used. A flow of 0.4 ml/min over a time of 16 min was performed. Mobile phases contain 5 mM ammonium acetate and 0.5 % acetic acid. Metabolites were stepwise eluted with 15 % ACN acetonitrile in the order shown in **Table 6**.

Table 6. Summary of the stepwise elution with 15% acetonitrile

Time [min]	Solvent B [%]
0	15
5	50
7	70
9	90
9.5	90
9.51	15
16	15

SIM signals were set to a negatively charged 147 (m/z) and 133 (m/z) positively charged fragment for cinnamic acid (elution time 5.7) and 316 (m/z) for cinnamic alcohol. After the incubation, the reactions were stopped by adding ~ 100 % methanol to the samples. After shaking and centrifuging, the supernatant was transferred into HPLC cuvettes for analysis.

3.10 GC-MS (Gas chromatography-Mass spectroscopy) analysis

The assay was carried out as follows: 473 μ l of 50 mM MES buffer, pH 7.5, containing 10 mM MgCl₂, 1 mM EDTA, 1 mM DTT and 24 μ l of substrate solution (pentanoic, hexanoic, or octanoic acid 100 mM in DMSO) were added followed by 30 μ l of CAR enzyme preparation (approximately 1-4 mg/ml for various enzymes), 36 μ l of NADPH (100 mM in ddH₂O), 36 μ l of ATP (100 mM in ddH₂O) and 1 μ l pyrophosphatase (3U/ μ l). Appropriate standards at concentrations of 100 mM, i.e. pentanoic, hexanoic, octanoic acid and corresponding aldehydes dissolved in DMSO were processed in parallel. The reaction proceeded at 28°C and 300 rpm in Eppendorf thermomixers for 2 h. The reactions were stopped by adding 10 μ l of 3 M HCl. An

Material and Methodes

equal reaction volume of ethyl acetate solution (0.01 % tetradecane as internal standard) was added and vigorously mixed. The upper phase containing ethyl acetate was then transferred to another tube and sodium sulphate (5-10% v/v) was added. After mixing, the supernatant was taken and transferred to glass tubes closed with a lid for the analytic GC-MS measurement. The analysis of aliphatic carboxylic acid reduction products was carried out with Chirasil-Dex 25 mm x 0.32 mm * 25 m GC column. The protocol was based on 2 ml/min flow and is summarized in **Table 7**.

Table 7. Protocol of the used temperature profile for the GC-FID analysis

	° C	Next °C	Hold [min]	Run time
Initial	-	40	5	5
Ramp 1	10	140	0	15
Ramp 2	20	160	7	23
Ramp 3		40	-	∞

3.11 Fermentation and purification procedure of *GkPPTase*

E. coli containing the pMS470_*GkPPTase* plasmid with the PPTase sequence of *G. kaustophilus* was cultivated in LB-media and was induced using 0.2 mM IPTG for the transcription at 37°C for 24 h. Cells were centrifuged for 10 min at 4000 rpm at 4°C. The cell pellet was resuspended in 25 ml CAR-Storage buffer and was sonicated for 6 min by a pulse of 80 %. The sample was centrifuged by using an Optima LE80K at 40,000 rpm for 45 min with the rotor type 70 Ti and 4 °C. The supernatant was heat-treated for 10 min at 70°C to denature other proteins than the potentially thermostable *GkPPTase*. A further centrifugation step for 10 min at 4000 rpm and 4°C separated the precipitated proteins from the desired *GkPPTase* in the supernatant. To assess the success of heat purification, the procedure was visualized by NuPAGE.

3.12 Pyrophosphatase (PPase) assay

To determine the influence of the pyrophosphate, which can inhibit aldehyde production, the HPLC analysis was performed. This assay contained 162 mM CAR-Storage buffer, 4 mM cinnamic acid, 0.35 mg/ml NcCAR and the same amount of pyrophosphatase from baker's yeast (Sigma) and, ultimately, 4 mM each of NADPH and ATP. As a reference the assay was

performed without pyrophosphatase and buffer was added instead. Samples were collected between 30 min and 240 min in 30 min steps and reactions were stopped with 200 µl methanol.

3.13 Influence of additional phosphopantetheinylation on the enzymatic activity of recombinant CARs

The phosphopantetheine transferase (PPTase) is necessary for the activation of CARs as described in the introduction. To examine the degree of CAR activation after expression in the presence of *Ec*PPTase, the enzyme preparations were treated *in vitro* with additional PPTase and CoA. *Ni*CAR was used as control, because this enzyme was not already activated. Only with additional CoA and PPTase *Ni*CAR should be active. Activities of treated samples were compared to the untreated blank reactions using the plate reader assay. The used substances and concentrations are shown in **Table 8**. *Nc*CAR and *Ni*CAR were incubated for 1 h at 28°C and measured over a time of 10 min at 28°C and a wavelength of 340 nm.

Table 8. Used compounds for the analysis of the enzyme activation.

Compound	Final concentration
CAR-storage buffer	80 mM
CoA	0.2 mg/ml
Enzyme 1:2	1.13 mg/ml
Enzyme 1:5	0.6 mg/ml
Enzyme 1:10	0.425 mg/ml
Additional PPTase	0.025 mg/ml
ATP	1 mM
NADPH	0.5 mM
Hexanoic acid	5 mM

4 Results

4.1 Expression and purification of NcCAR

9.8 g wet cells were produced by the fermentation procedure as described in 3.3. Based on the method described in 3.3, a gradient purification of the NcCAR was performed. The purification procedure was monitored by UV-spectroscopy. 2.2 g wet cells were treated as described in 3.4. Approximately 30 ml of supernatant after ultracentrifugation were loaded onto two subsequent HiTrap™ FF 5 ml columns. The UV-curve started out of range and declined under 20 mAU over 60 ml. The elution was started with linear increase of the buffer-B content after 60 ml. The UV-peak containing the NcCAR started to appear at 70 ml. A small shoulder appeared during the elution step over a total volume of 30 ml. The climax occurred at 85 ml. Protein elution ended after a total volume of ~ 100 ml (**Figure 5**).

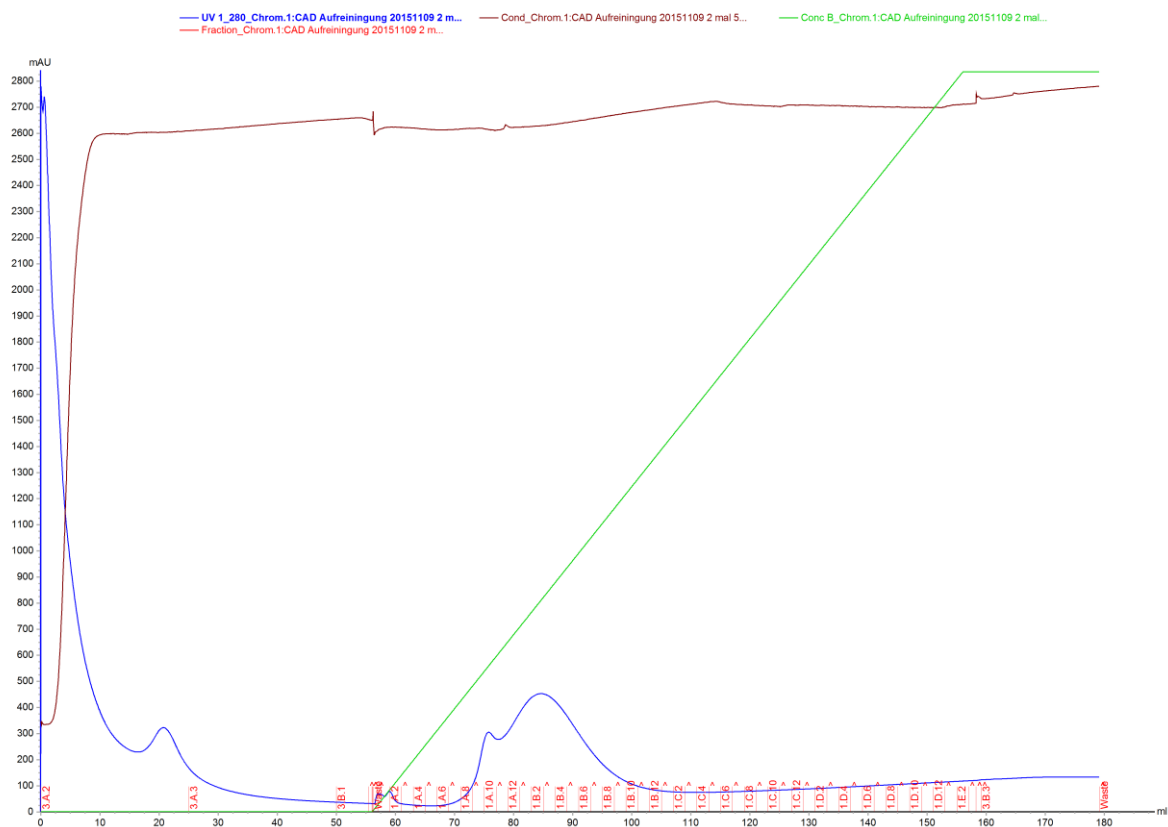


Figure 5. Chromatogram of the first purification of NcCAR using a gradient from 0 % buffer-B to 100 % buffer-B over 10 CV. 2 ml samples were collected.

Results

The buffer exchange of the collected fractions containing the *NcCAR* was executed with a HiPrepTM 26/10 Desalting column on an ÄKTA prime (**Figure 6**).

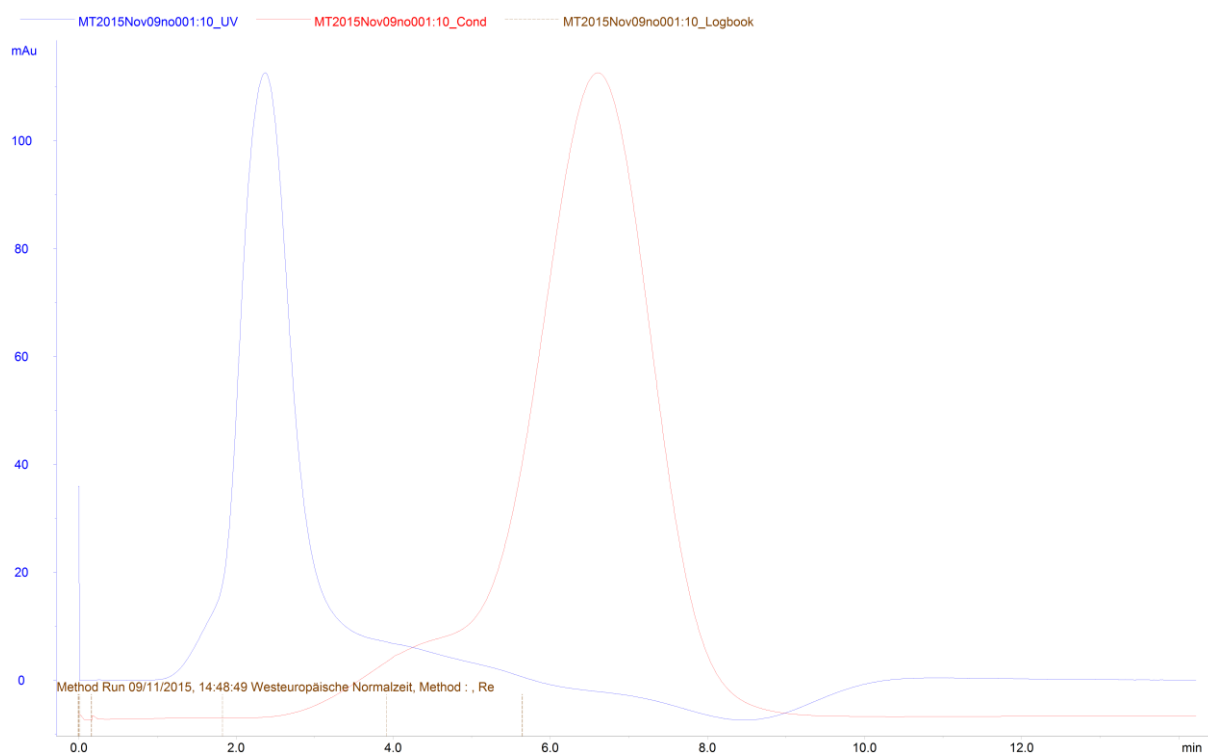


Figure 6. Screenshot of the rebuffering using a HiPrepTM 26/10 Desalting column. The blue curve describes the UV-absorption, the red curve the conductivity.

Results

For the buffer exchange, a flow of 2 ml/min was used. The imidazole was separated from the proteins. The collected samples were concentrated using a Vivaspin 20 centrifugal concentrator (cut-off 30 kDa) up to ~ 11.85 mg/ml as measured with a Nanodrop 2000c Spectrophotometer (7.1.7). 10 % Glycerol were added to 500 μ l aliquots of the purified protein. The aliquots were shock-frozen in liquid nitrogen and were stored at -80°C . The SDS-PAGE in **Figure 7** shows the quality of the gradient purification procedure.

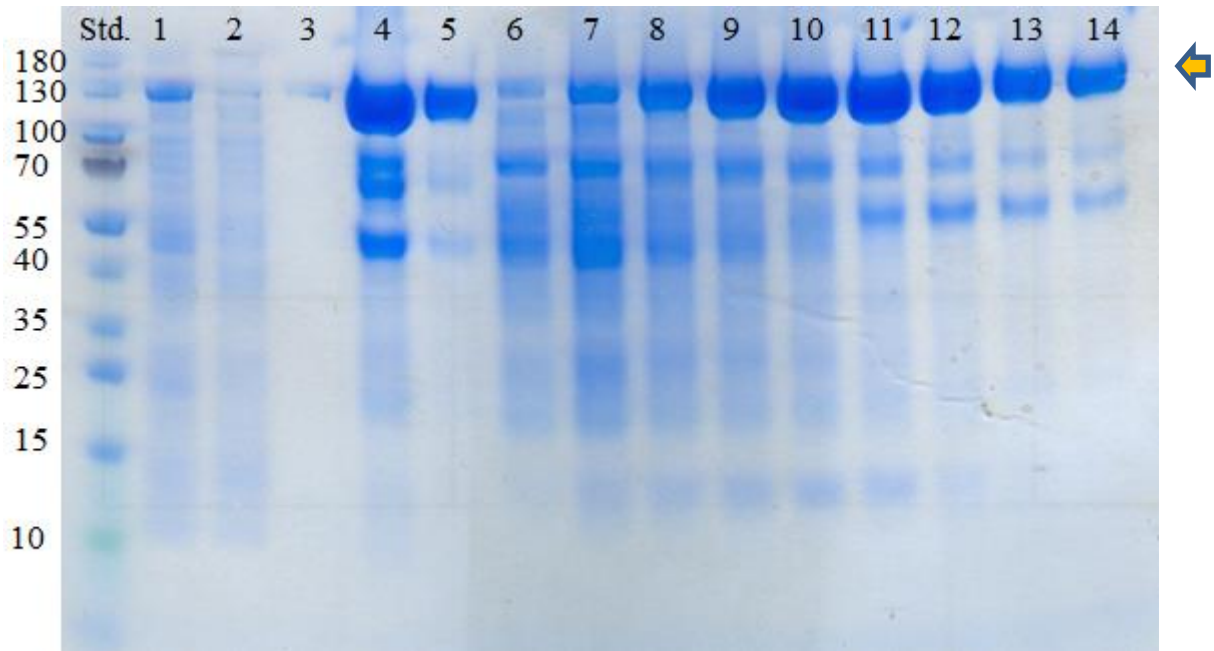


Figure 7. SDS 4-12 % Bis-Tris-gel of the different fractions of protein purification by Ni-affinity chromatography. Page Ruler Prestained Protein Ladder (10-180 kDa) was used as standard. Slot 1 contains the load, slot 2 contains the flow-through. Slot 3 wash. Slot 4 and 5 contain the pooled fractions. Slot 6 – 14 contain the different collected fractions. *NcCAR* should appear by 120 kDa (orange arrow).

The collected *NcCAR* preparation was not of very high purity (see slot 4 and 5). Three prominent bands of unknown proteins between 40 kDa – 70 kDa were detected, as well as other background proteins.

Results

To improve the purification of *NcCAR*, a stepwise elution protocol was established. Three steps with an imidazole concentration of 20 mM, 85 mM and 500 mM were performed. The chosen steps were based on the experience which were gained during the gradient purification. The same wet weight of cells (2.2 g) was used for the purification. With an additional step of 20 mM imidazole, the shoulder could be separated into two different peaks (**Figure 8**).

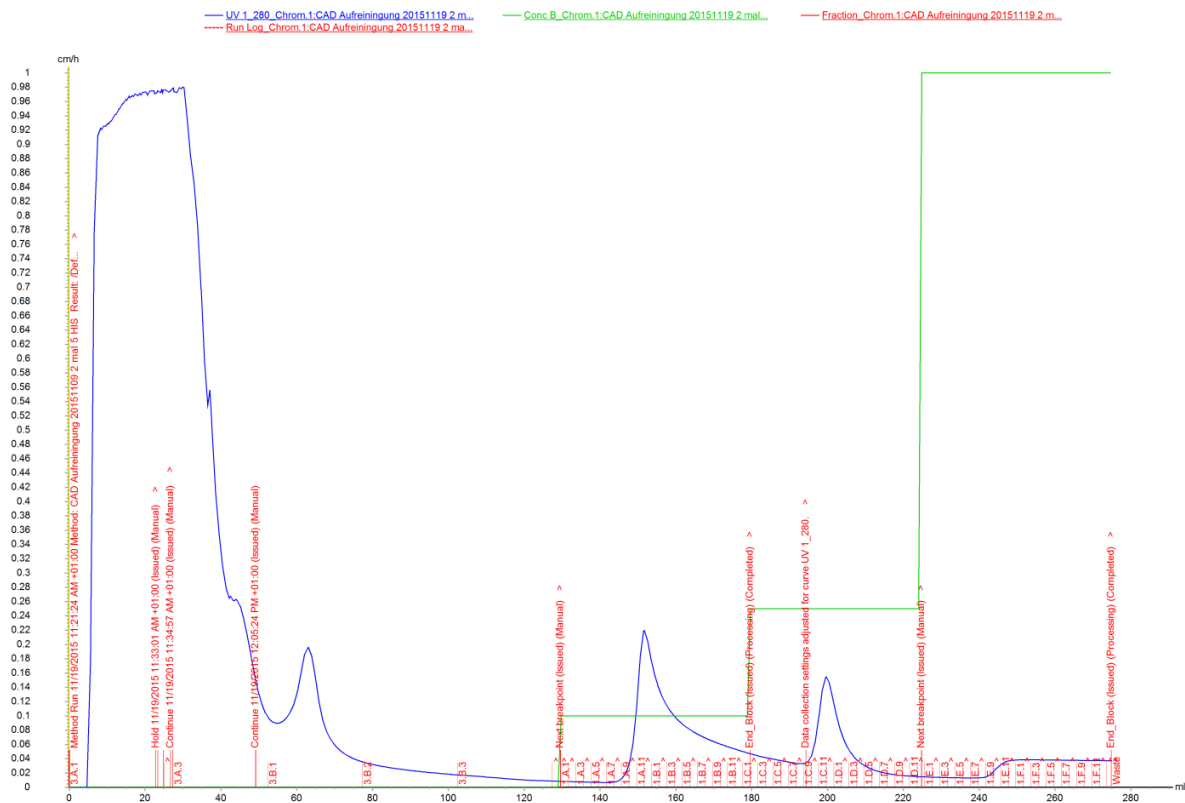


Figure 8. Chromatogram of the stepwise purification of *NcCAR* using three steps of buffer-B (10 %, 25 %, 100 %) over 10 CV. 2 ml samples were collected.

The UV-signal increased while the protein was loaded to the column in the range between 10 ml to 80 ml. The signal of the first peak corresponds to proteins which did not bind to the column. The elution started at 125 ml. The first elution step with an imidazole concentration of 20 mM removed proteins showing weak interaction with the column. This elution fraction was defined as the first peak. A tailing UV-absorption was detected after the first elution step with 20 mM imidazole after 145 ml. The second elution step containing an imidazole concentration of 85 mM started at 180 ml. The corresponding UV-peak was detected with a maximum intensity of 450 mAU and was classified as the second elution peak. After the UV-absorption decreased, the final step with an imidazole concentration of 500 mM was performed.

Results

The collected fractions of the two peaks were pooled and the buffer was exchanged as described in 3.4 with the unicorn procedure. The run was performed with CAR-Storage buffer with a flow-rate of 3 ml/min. The desalted flow through between 6 min and 8 min was collected (Figure 9).

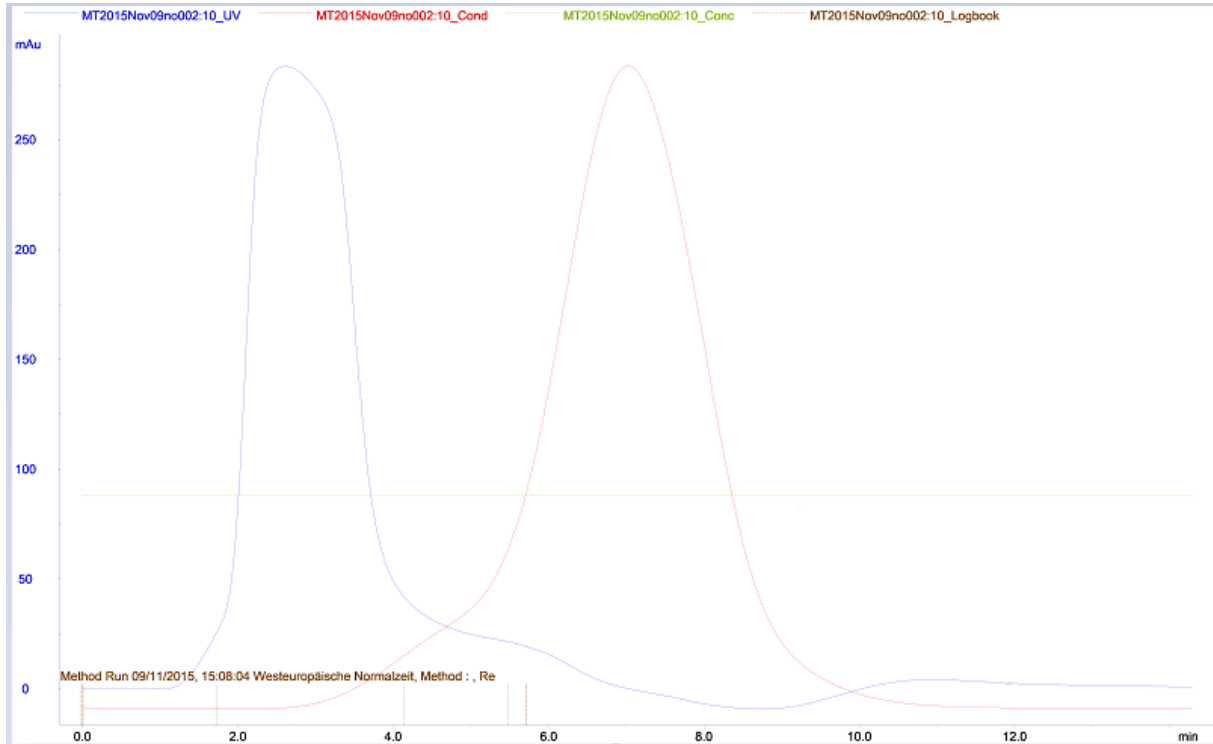


Figure 9. Buffer exchange by

The collected pools were concentrated using a Vivaspin 20 centrifugal concentrator. About 13.49 mg/ml protein was purified and 500 μ l aliquots upon addition of 10% glycerol were stored at -80°C .

The SDS-PAGE in **Figure 10** shows the quality of the gradient purification procedure.

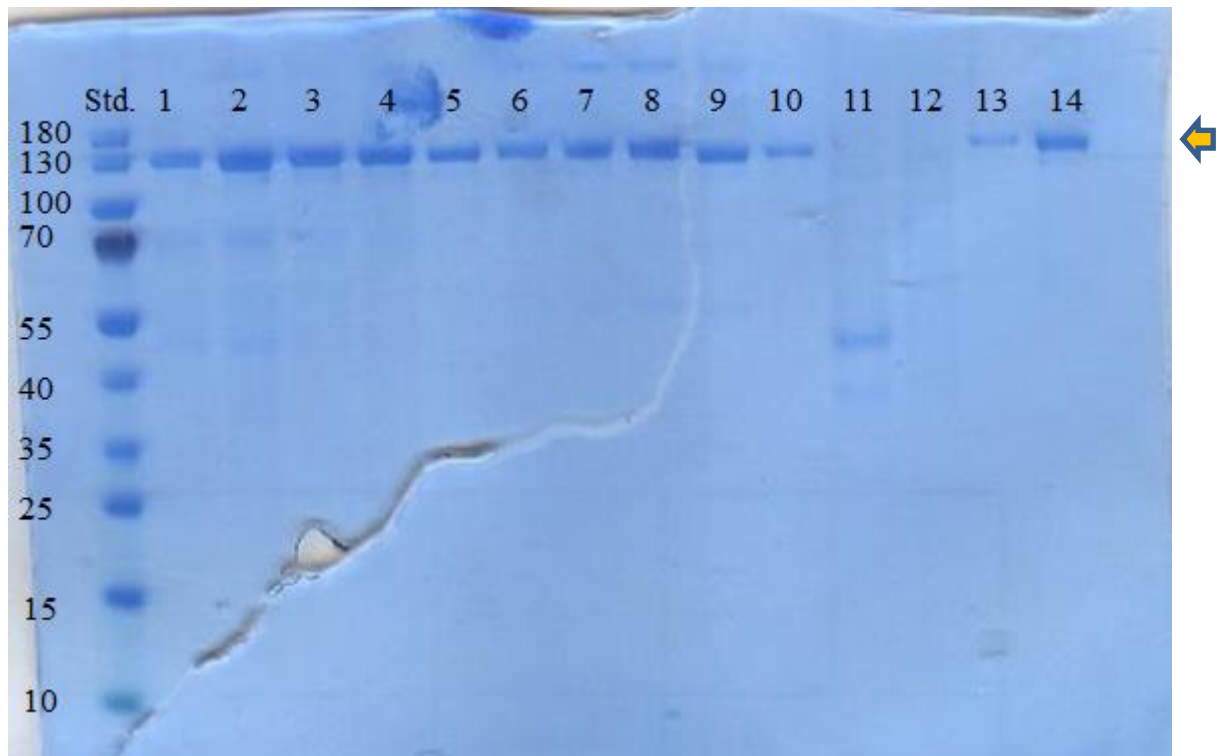


Figure 10. SDS 4-12 % Bis-Tris-gel of the different fractions of the protein purification with Ni-affinity chromatography. PageRuler Prestained Protein Ladder (10-180 kDa) was used as standard. Slot 1 - slot 10 show the collected fractions of the purification. Slot 11 shows the final pooled samples of the last purification step with 500 mM imidazole. Slot 12 consists of the flow-through (1:10 diluted). Slot 13 shows the first pooled purification peak. Slot 14 contains the second pooled peak (1:10 diluted) which were collected during the elution steps. *NcCAR* should appear by 120 kDa (orange arrow).

Impurities appeared in the single collected fractions between 40 and 70 kDa between slot 1 and 10. The flow-through contained bands in the range of 35 – 180 kDa. Slot 11 showed protein bands of 45 kDa. In slot 13 some impurities could be detected as well as for slot 14 which represented the second elution step with 85 mM imidazole. To improve the purity of the enzyme preparation, an additional gel-filtration step was established as described in chapter 3.4.

The SDS-PAGE in **Figure 11** shows the quality of the different purification procedures. The first slot contained the cell free extract (1:2 diluted), with different protein bands over the range of the used marker. Slot 2 with the treated cell pellet contained the total protein of the organism. The first purification step (**Figure 7**) is shown in slot 4, by using the His-Tag. *NcCAR* was enriched, compared to slot 1 and 2. An intensive band at 130 kDa correlated to the expected size of *NcCAR*. Slot 5 showed the result of the second purification procedure after removal of the His-Tag. Still, some impurities yielding in protein bands between 35 and 100 kDa were

present. Slot 6 contained the final gel-purified material which included less impurities and an intensive band by 130 kDa.

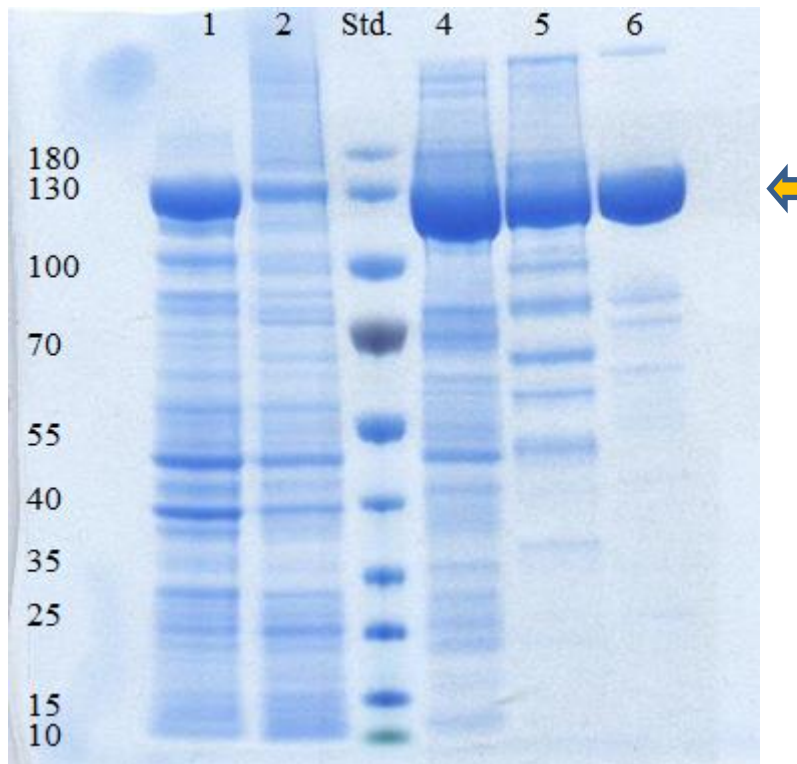


Figure 11. SDS 4-12 % Bis-Tris-gel of different purification steps with *NcCAR* after 1 h run time on 200 V in MOPS-buffer. Slot 1: Soluble fraction of the cell free extract. Slot 2: cell pellet in 6 M urea. Slot 3: PageRuler Prestained Protein Ladder (10-140 kDa). Slot 4: Purified enzyme upon Ni-affinity chromatography. Slot 5: *NcCAR* after removal of the His-Tag with *TEV*-protease and a further purification with Ni-affinity chromatography. Slot 6: Gel-filtered protein after the first purification with Ni-affinity chromatography. Staining with SimplyBlue™ SafeStain solution overnight. Bleached with ddH₂O overnight. Orange arrow indicates the *NcCAR*.

4.2 Results of the *NiCAR* purification

NiCAR was purified as described in chapter 3.5 (**Figure 12**). The first elution pool slot 7 contained some impurities between 40 and 100 kDa. Those became less in the second purification pool: Slot 9, where just one band appeared around 130 kDa which correlated to the size of the *NiCAR*. In comparison to *NcCAR*, the one step Ni-affinity purification resulted in a preparation of higher purity.

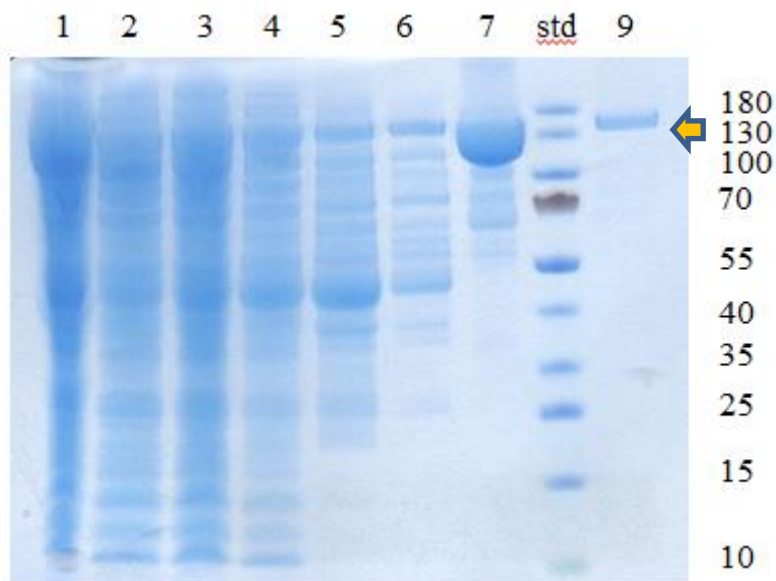


Figure 12. SDS 4-12 % Bis-Tris-gel of the *NiCAR* purification after 1 h run time at 200 V in MOPS-buffer. Slot 1 contains the load, slot 2 and 3 flow-through, slot 4, 5, 6 wash steps 1-3. Slot 7 the *NiCAR* elution pool. Page Ruler Prestained Protein Ladder (10-180 kDa) was used as standard in slot 8. Slot 9 shows the second elution pool. Orange arrow indicates the *NiCAR*.

4.3 Results of the PPTase purification

The PPTase purification procedure was realised as described in chapter 3.5. The pool containing the PPTase was loaded in slot 6. Some impurities appeared between 180 and 40 kDa. An intensive band occurred at 35 kDa, which correlated to the expected protein size. The purified enzyme preparation of Margit Winkler will not be used in the future because of too many impurities (**Figure 13**).

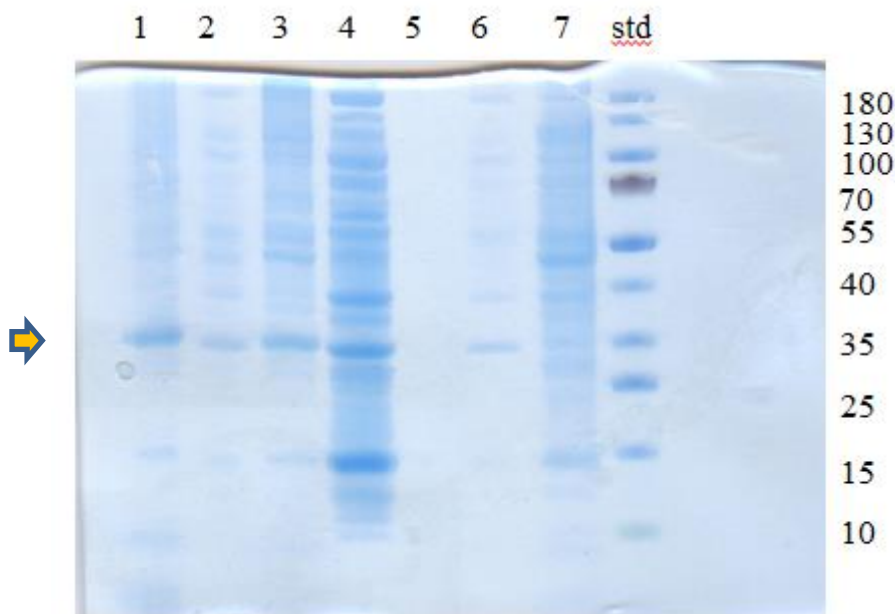


Figure 13. SDS 4-12 % Bis-Tris-gel of the pMS470_GK PPTase after heat treatment, for 10 min at 70°C, at a 1 h run time at 200 V in MOPS-buffer. Slot 1 pellet of insoluble fraction after sonication and centrifugation treated with 6 M urea, slot 2 supernatants after sonication and centrifugation, slot 3 pellet treated with 6 M urea, slot 4 old stored fermentation of PPTase treated with 6 M urea, slot 5 empty, slot 6 PPTase pool of the new 20 ml fermentation, slot 7 whole cells treated with 6 M urea, PageRuler Prestained Protein Ladder (10-180 kDa) has been used as standard in slot 8. The PPTase has ~35 kDa (yellow arrow).

4.4 Results of the substrate screening with *NcCAR*

To analyse enzyme activity, the depletion of NADPH by *NcCAR* was followed over a time of 10 min at 28°C and a wavelength of 340 nm using the Synergy MX-plate reader. NADPH depletion is an indirect way to monitor the reduction reaction. The assay was performed under the conditions mentioned in chapter 3.8. To determine the standard error, all experiments were carried out in a minimum of biological duplicates and technical quadruplicates in UV-Star 96 well plates. **Figure 14** gives the results correlated to the length of the hydrocarbon chain. Cinnamic acid was measured in every reaction as a control of the enzyme activity.

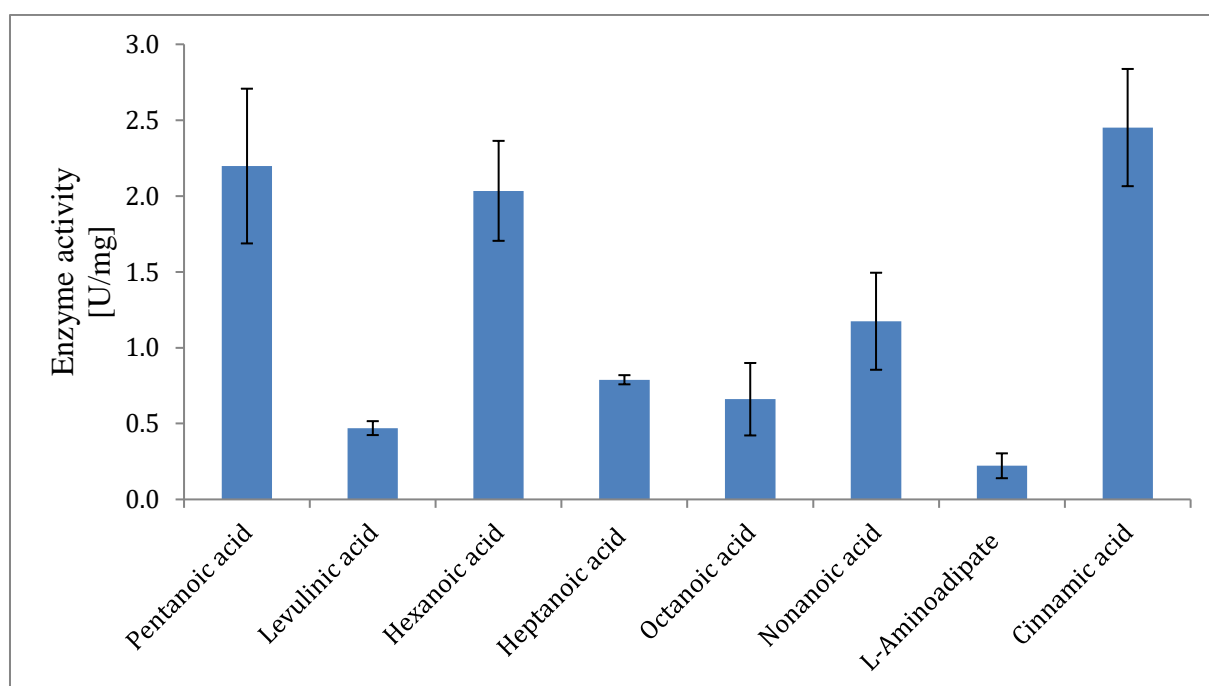
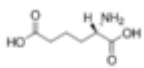
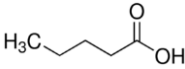
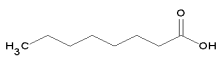
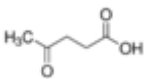
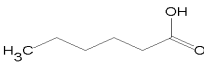
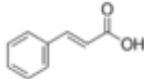


Figure 14. Overview of the aliphatic acids and cinnamic acid, and the respective enzyme activities. The standard error is given. The assay was based on the NADPH consumption over time.

The highest enzyme activity was measured with pentanoic acid and hexanoic acid. The average of the enzyme activities for these two substrates constituted 2.2 U/mg, respectively 2.0 U/mg. The lowest enzyme activity was determined for L-Aminoadipate and levulinic acid. (Table 9) summaries the used aliphatic substrates and their structural formula.

Table 9. Overview of the aliphatic substrates used and the structural formula obtained from Sigma Aldrich homepage 20.09.2016. Cinnamic acid was used as reference to control the enzymatic activity.

Substrate	Structural formula	Substrate	Structural formula
L-2-Aminoadipate		Heptanoic acid	$\text{CH}_3(\text{CH}_2)_4\text{CH}_2\text{COOH}$
Pentanoic acid		Octanoic acid	
Levulinic acid		Nonanoic acid	$\text{CH}_3(\text{CH}_2)_6\text{CH}_2\text{COOH}$
Hexanoic acid		Cinnamic acid	

4.5 Verification of aldehyde production by GC-FID

Using GC-FID analysis, based on the conditions mentioned in chapter 3.11, a direct enzyme assay was performed. Pentanoic, hexanoic and octanoic acid were analysed as described. The result illustrated in **Figure 15** as an additional proof for aldehyde production by *NcCAR*. Pentanoic acid as substrate was not converted that effectively. A lot of acid was retained after the reaction process. However, it showed a slightly higher aldehyde concentration than the other substrates. Except for the pentanoic acid, alcohol was found in all of the performed analyses.

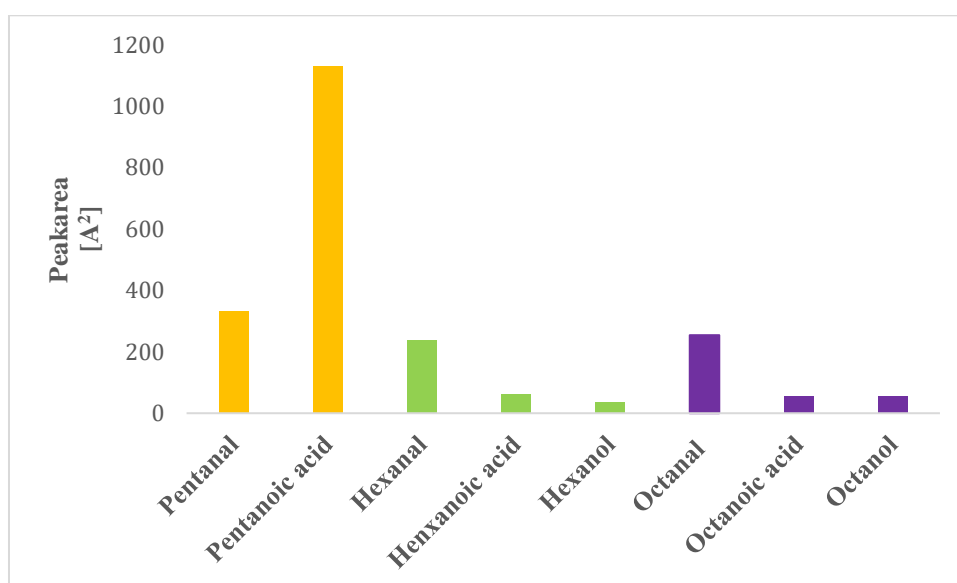


Figure 15. Result of the GC-FID measurement of pentanoic, hexanoic and octanoic acid conversions.

In addition to the aliphatic substrate screening, the assay was performed also for aromatic acids (**Figure 16**). Cinnamic acid was measured in every treatment to control the enzyme activity.

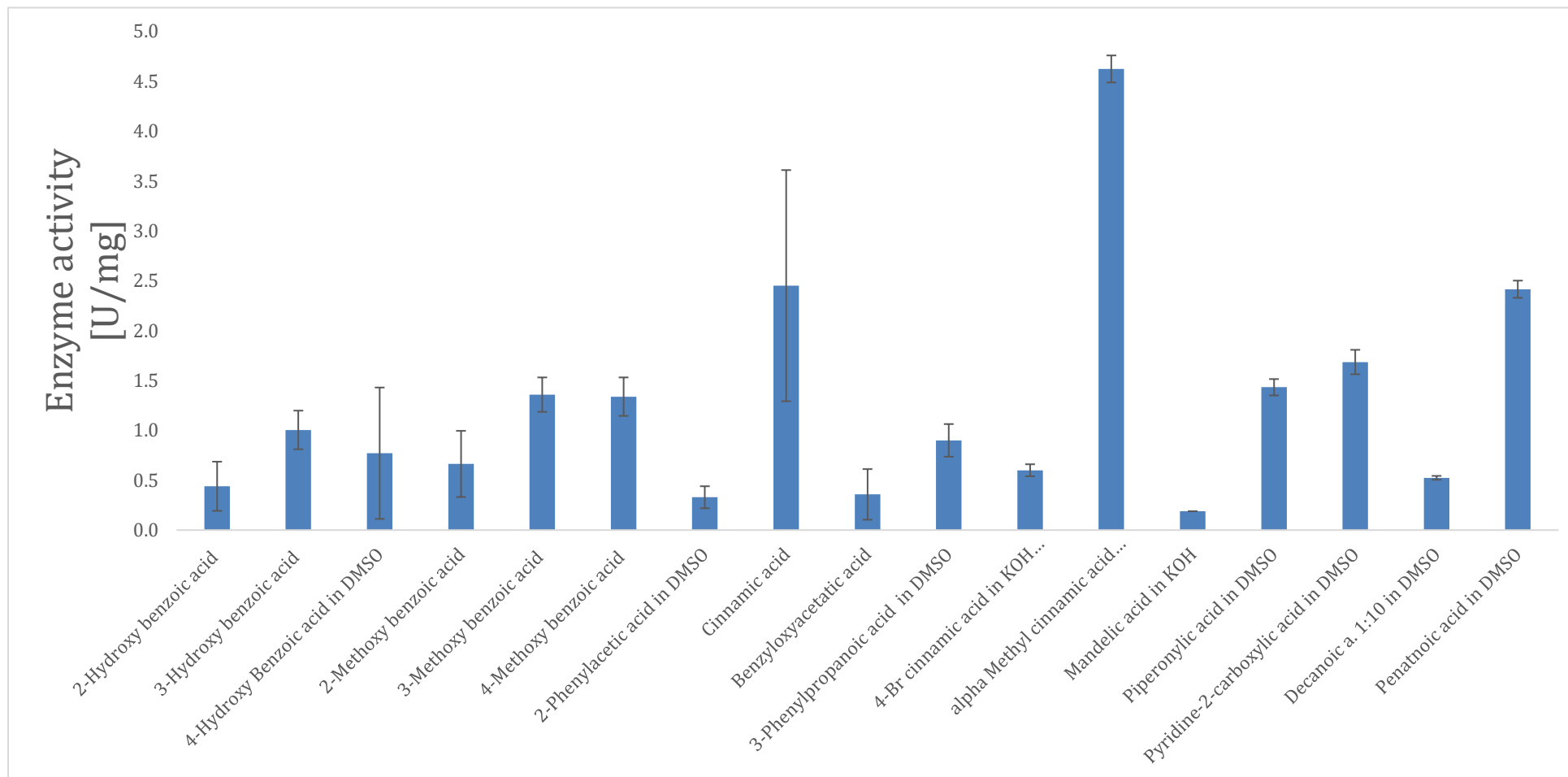
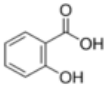
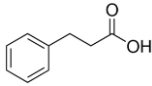
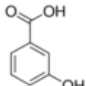
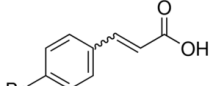
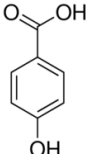
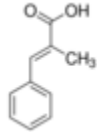
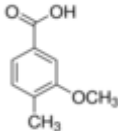
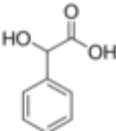
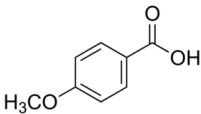
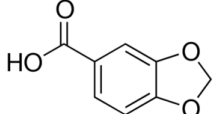
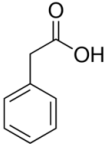
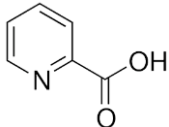
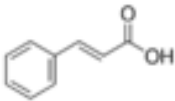
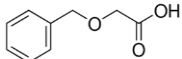


Figure 16. Examination of the enzyme activity for aromatic acids. Cinnamic acid was added in each assay as a control for the enzyme activity. The standard error is given. The assay was based on the NADPH consumption over time.

The highest enzyme activities of 4.62 U/mg were found for α -methyl cinnamic acid as substrate. Secondly, cinnamic acid and pentanoic acid were converted with enzyme activities of 2.5 U/mg and 2.2 U/mg performing well compared to the other substrates. The lowest activity was obtained for mandelic acid as substrate. Table 10 contains the aromatic substrates used and the corresponding structural formula.

Table 10. Overview of the aromatic substrates used and the structural formula obtained from Sigma Aldrich homepage 20.09.2016.

Substrate	Structural formula	Substrate	Structural formula
2-Hydroxy benzoic acid		3-Phenylpropanoic acid	
3-Hydroxy benzoic acid		4-Bromocinnamic acid	
4-Hydroxy benzoic acid		α -Methyl cinnamic acid	
2-Methoxy benzoic acid		Mandelic acid	
4-Methoxy benzoic acid		Piperonylic acid	
2-Phenylacetic acid		Pyridine-2-carboxylic acid	
Cinnamic acid			
Benzyloxyacetatic acid			

The co-solvent tolerance screening was performed as described in chapter 3.8. DMSO and methanol were compared to analyse the impact of possible solvents for the substrates as mentioned in 3.8 (**Figure 17**).

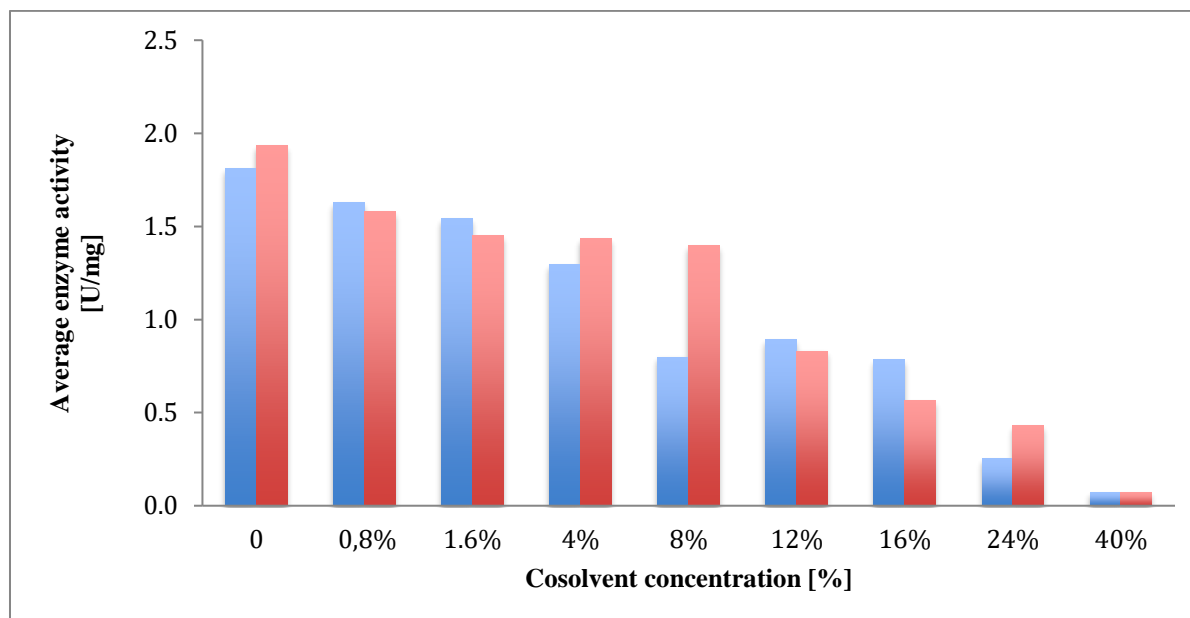


Figure 17. Co-solvent tolerance screening with methanol (red) and DMSO (blue). The concentrations in % refer to the total volume of the assay (200 μ l). The assay was performed two times under the same conditions.

The highest enzyme activity was detected without the use of any co-solvent at an activity of 1.8 U/mg for DMSO and 1.9 U/mg for methanol. This slight deviation may be traced back on the protein concentration measurement, using the NanoDrop device. Up to a concentration of 8 % the impact of the used co-solvents increased. At a co-solvent concentration of 8 % the enzyme activity diminished by ~ 29 %. At the highest concentration of the co-solvent (40 %), the enzyme activity constituted less than ~ 0.07 U/mg.

4.6 The optimal pH conditions for *NcCAR*

Different buffer systems in their concentration of 100 mM buffer with 10 mM MgCl₂ were established to determine the best buffer conditions for the enzyme. The assay was performed under the conditions mentioned in chapter 3.8. All pH ranges were calculated by the bioinformatics.org webpage²⁵. In total, the range between pH 3.5 up to pH 10 was analysed. The results are summarised in **Figure 18**.

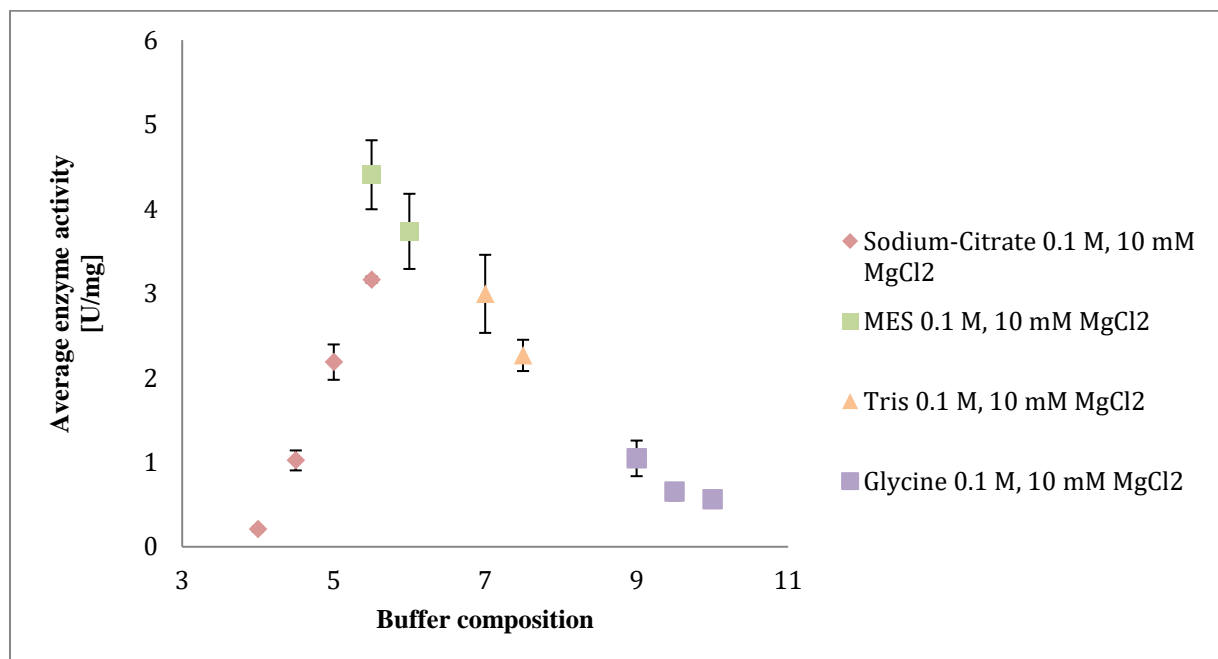


Figure 18. Buffer-screening in the range of pH 3.5 up to pH 10.0. All buffer compositions are concentrated 0.1 M and contained 10 mM MgCl₂ to generate Mg-ATP-complexes.

The first pH range was performed with sodium citrate between pH 3.5 and pH 5.5. Enzyme activity increased with the pH value up to 3.2 U/mg. Using MES-buffer in the same pH scope (pH 5.5), the highest activity of 4.4 U/mg was determined. With even higher pH values, enzyme activity decreased to 0.6 U/mg at pH 10.0.

To confirm these results, which were in contradiction to the literature,^{4,5} the buffer screening was repeated and was analysed by the use of HPLC. The advantage of this method was to gain direct information about the amounts of the generated aldehyde and alcohol upon converting known substrate concentrations. The results are summarized in **Figure 19**, comparable to those of the plate reader. The highest enzyme activity and aldehyde production occurred in the range

Results

of pH 5 to pH 7. In the range of pH 4 to pH 4.5 there was no production of cinnamaldehyde. Above pH 7.5 the enzyme activity decreased.

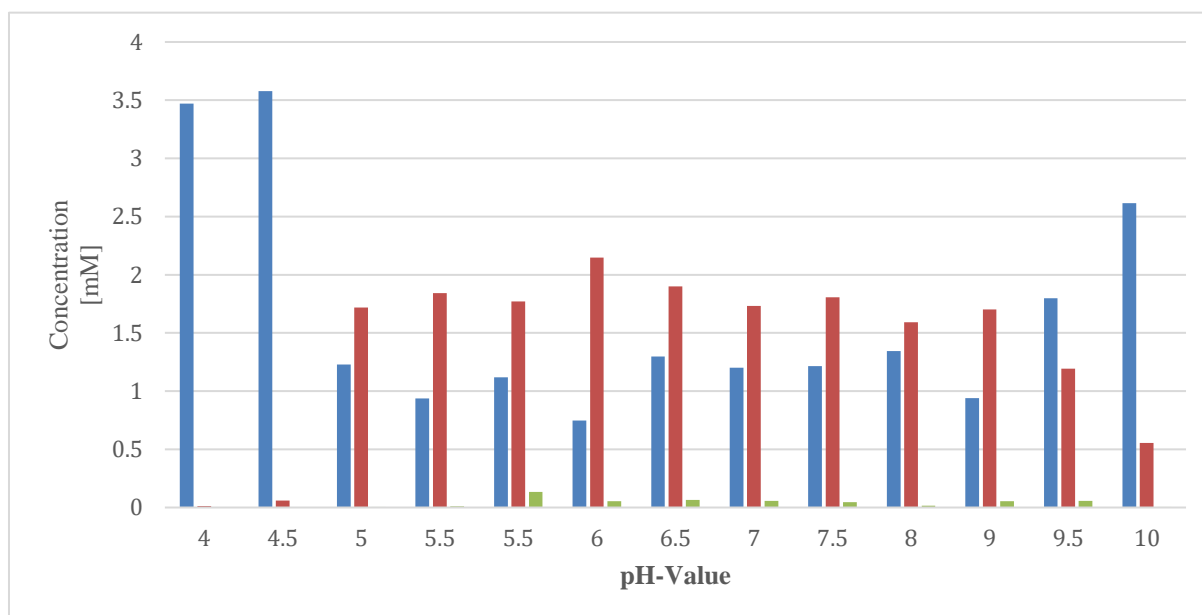


Figure 19. HPLC screening of the pH optimum of *NcCAR*. The amount of cinnamic acid, produced aldehyde and alcohol was measured in the pH range between pH 4 to pH 10. The blue bars show the acid concentration, the red ones illustrate the aldehyde concentration and the green ones the alcohol concentration.

4.7 Optimal temperature for *NcCAR* mediated carboxylate reduction

To determine the temperature optimum for enzyme activity, the temperature range between 20°C and 65°C was analysed in 5°C increments under the conditions mentioned in chapter 3.8. The buffer compositions and pH approach based on the calculations of the bioinformatics.org webpage²⁵. Because the Synergy MX-Plate reader is not able to cool down below 20°C or heat up over 65°C, the range was defined as such (**Figure 20**).

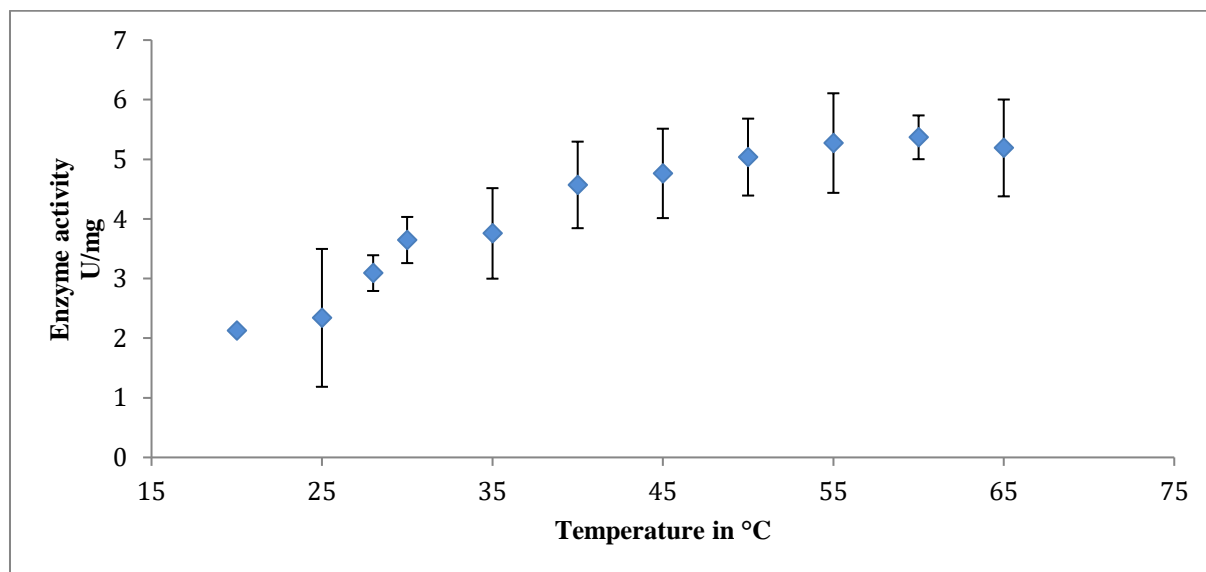


Figure 20. Results of the temperature determination for the best assay conditions. Cinnamic acid was used as substrate. The Synergy MX-Plate reader was preheated until the temperature was reached.

The first temperature of 20°C resulted in an enzyme activity of 2.13 U/mg. By increasing the temperature, the activity increased as well. At the temperature of 60°C, the highest activity of 5.37 U/mg was observed. Between the temperatures of 40°C up to 65°C the enzyme activity behaved almost identically.

4.8 Temperature stability of the enzyme

To determine the temperature stability of the enzyme, the protein was incubated for 1.5 h at different temperatures in the range between 0°C up to 70°C. The residual activity of *NcCAR* was determined under the conditions mentioned in chapter 3.8 (**Figure 21**).

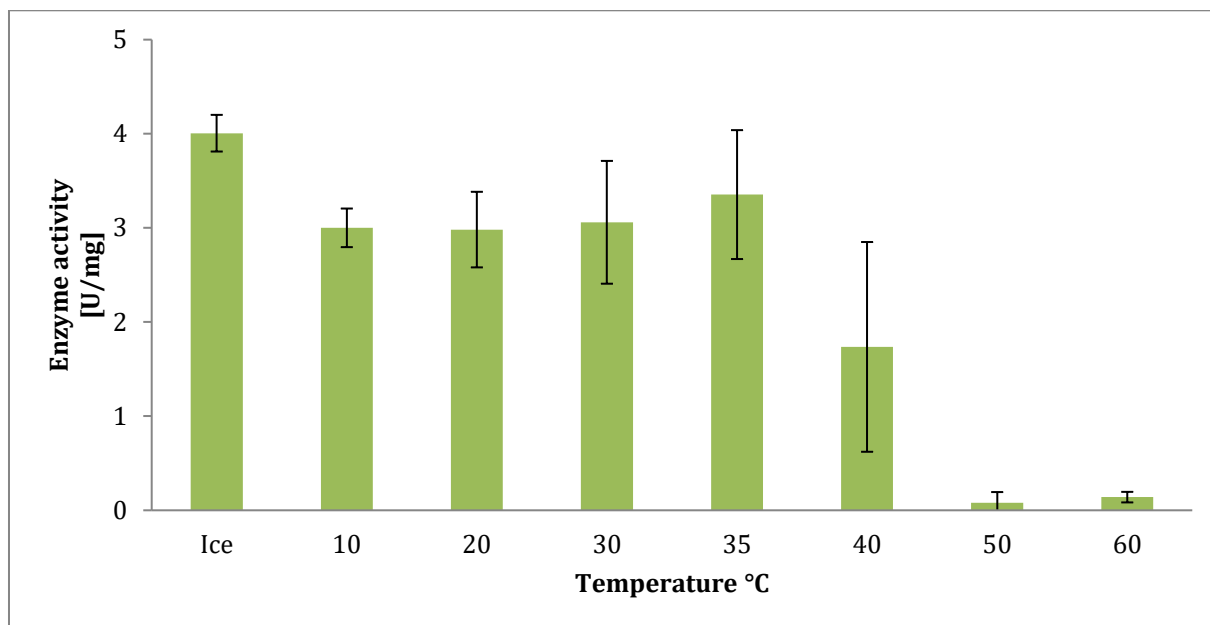


Figure 21. Result of the temperature stability of the *NcCAR*. The enzyme was incubated for 1.5 h at the corresponding temperature. The assay was performed with cinnamic acid as substrate at 28 °C.

The highest activity of 4.0 U/mg was determined upon incubating the enzyme for 1.5 h on ice. Between the temperatures of 10°C and 35°C the activity was stable in the average range between 2.98 U/mg and 3.4 U/mg. At temperatures higher than 50°C the enzyme became inactive.

4.9 Results of the enzyme kinetics.

As described in chapter 3.8 the enzyme kinetics was recorded. On the x-axis, 1 was divided by the substrate concentration [mM] and plotted with the calculated average of enzyme activity [U/mg]. The standard deviation was added. The result of the sigma plot calculation is illustrated in **Figure 22**, which shows a maximal velocity (V_{\max}) of 16.59 mM/min and the Michaelis constant (K_M) of 1.732 mM.

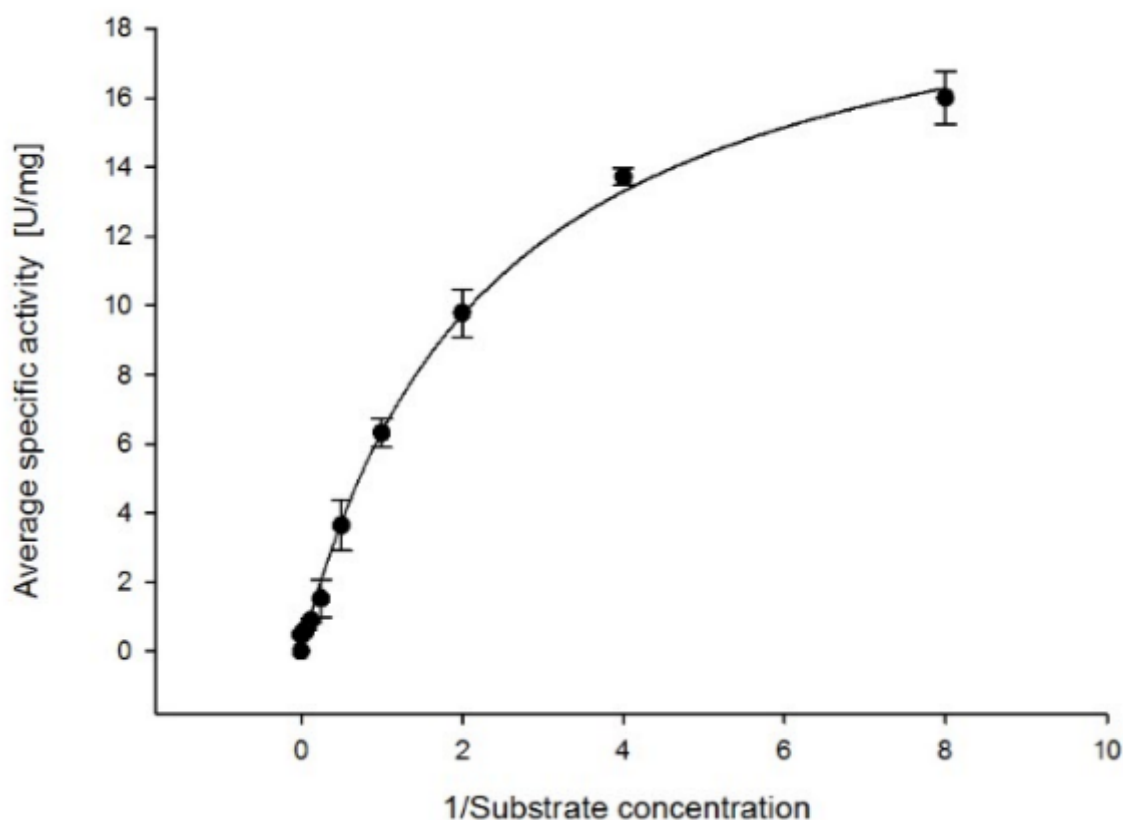


Figure 22. Result of the best fitted sigmaplot solution. Cinnamic acid was used as substrate in technical triplicates. The maximal velocity was 16.59 mM/min and the Michaelis Menten constant was 1.732 mM.

4.10 Phosphopantetheine transferase assay

The phosphopantetheine influence was analysed as described in chapter 3.13. The percentage enzyme activity is given. Different enzyme dilutions of *NcCAR* and *NiCAR*, i.e. 1:2, 1:5, 1:10, were prepared. The results are summarised in **Figure 23**. The enzyme activity was slightly increased compared to the already activated *NiCAR* by the addition of PPTase and CoA. At higher dilutions, the total enzyme activity dropped to ~ 75%. *NcCAR* showed in all samples a slightly higher activity than *NiCAR*.

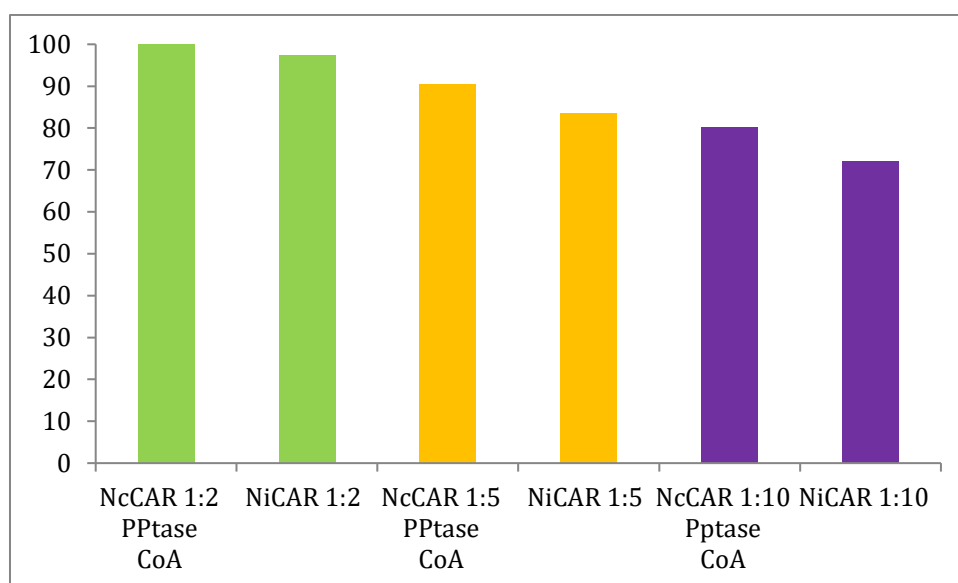


Figure 23. Result of the influences of the phosphopantetheine transferase of already activated *NcCAR* compared to *NcCAR* and *NiCAR* with additional PPTase and CoA to make sure that the whole enzyme was activated. Three different dilutions were analysed with hexanoic acid as substrate.

4.11 Influence of pyrophosphate

The influence of the pyrophosphate on the enzymatic reaction was analysed by preparing samples containing pyrophosphatase (PPase) and samples without PPase, as described in chapter 3.12. Every 30 min, samples were collected and the reactions were interrupted by adding 200 μ l methanol over a total time of 240 min. These samples were analysed by HPLC and the calculated concentrations are illustrated in the following figures.

In **Figure 24**, the results without PPase are summarised. The aldehyde concentration increased from 0 to 1.5 mM over a time of 30 min. The maximum conversion was reached at 4 mM substrate. After the first 30 min, the aldehyde concentration increased slowly to a final concentration of 1.7 mM. A decrease of the acid concentration was estimated in parallel. It started at 4 mM and dropped to a final concentration of \sim 2 mM. During the first interval of 60 min, the reduction of acid was higher, compared to the second interval between 60 min and 240 min. The amount of generated alcohol was close to 0 mM.

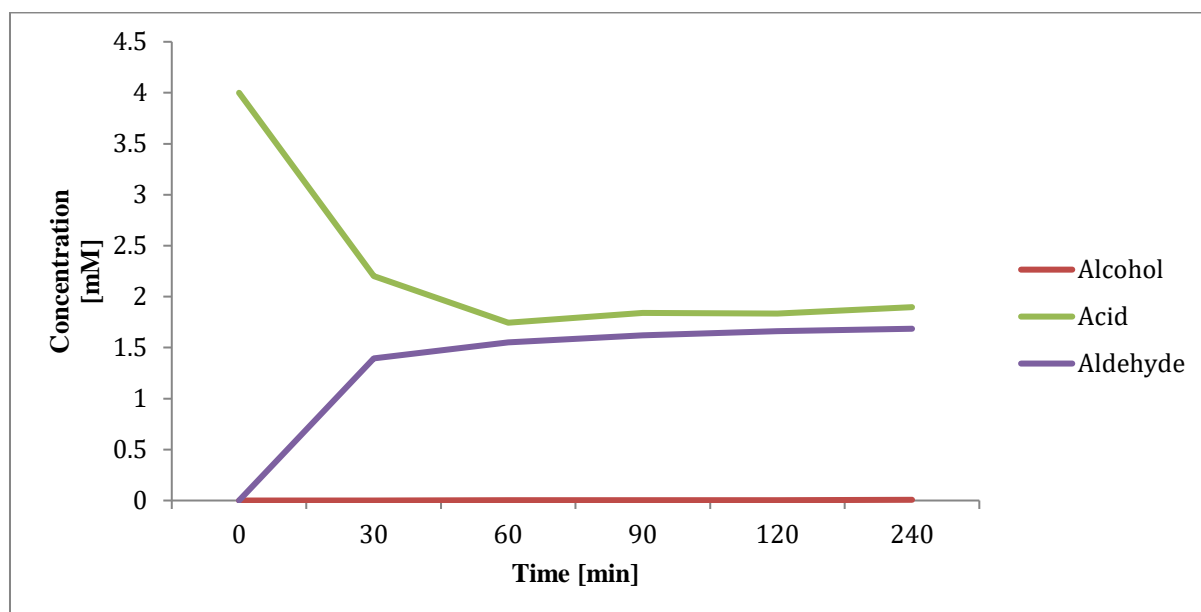


Figure 24. Time course of alcohol, acid and aldehyde concentrations without PPase over a time of 240 min.

During the second experiment, PPase was added to the samples. A huge influence could be detected concerning the generated aldehyde concentration which increased up to 3 mM over a time of 90 min. The highest production rate of aldehyde was observed between 0 and 60 min. After 90 min, the reaction slowed down. The acid concentration reduced in parallel to the generated aldehyde concentration. The production of alcohol could not be observed, as shown in **Figure 25**.

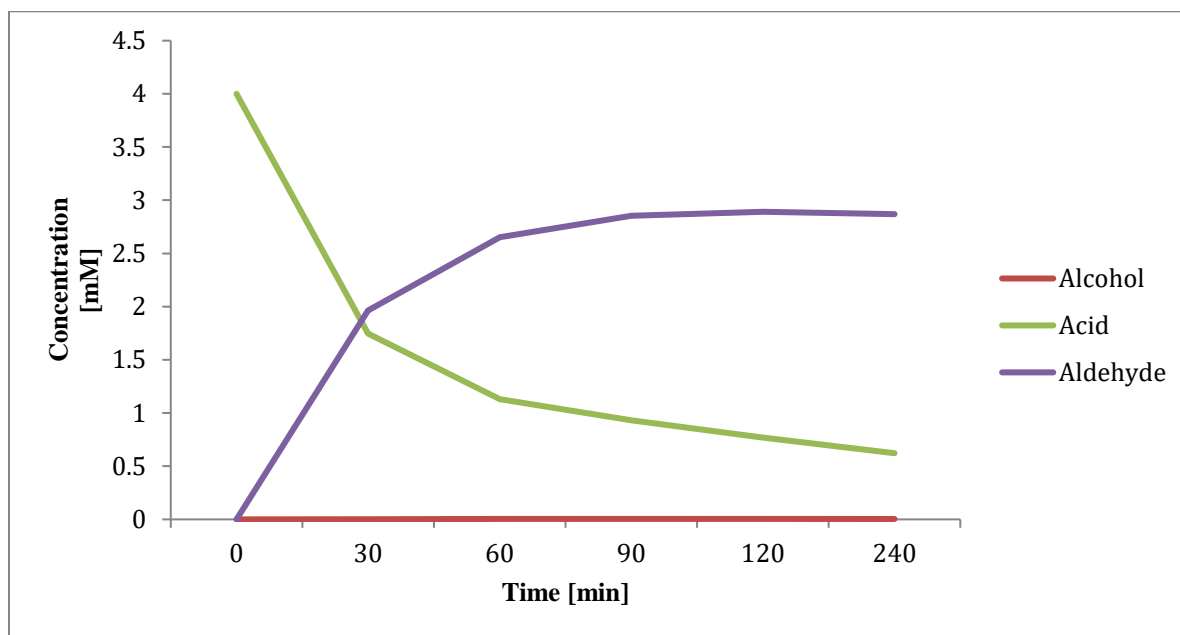


Figure 25. Time course of alcohol, acid and aldehyde concentrations with additional PPase over a time of 240 min.

Another pyrophosphate experiment was done with an immobilised enzyme preparation. *NcCAR* was attached to His TrapTM FF column (5 ml) material which was treated with Ni-sulphate. Samples were taken after 10, 30, 60 and 120 min and were analysed with HPLC as described in chapter 3.10. The acid concentration decreased over 120 min from 2.3 mM to 1 mM. Additionally, the aldehyde concentration rose from 0.3 mM after 10 min to 0.9 mM after 120 min as well as the alcohol concentration, which started at 0.1 mM (10 min) and ended at 0.34 mM (120 min). After 2 h, the immobilised catalyst was removed from the reaction supernatant, washed with buffer (in order to remove potentially inhibiting pyrophosphate) and was used for a second reaction cycle. In the second round, after the pyrophosphate was completely removed, the same results were obtained. Only the starting concentrations were increased. The acid concentration started at 3.2 mM at the 10 min mark and declined over 120 min to 2.3 mM. Similarly as in the first treatment, the aldehyde concentration increased from 0.4 mM (10 min) up to 0.95 mM (120 min). The alcohol concentration started at 0.1 mM and ended at a concentration of 0.45 mM. The HPLC results were illustrated in **Figure 26**.

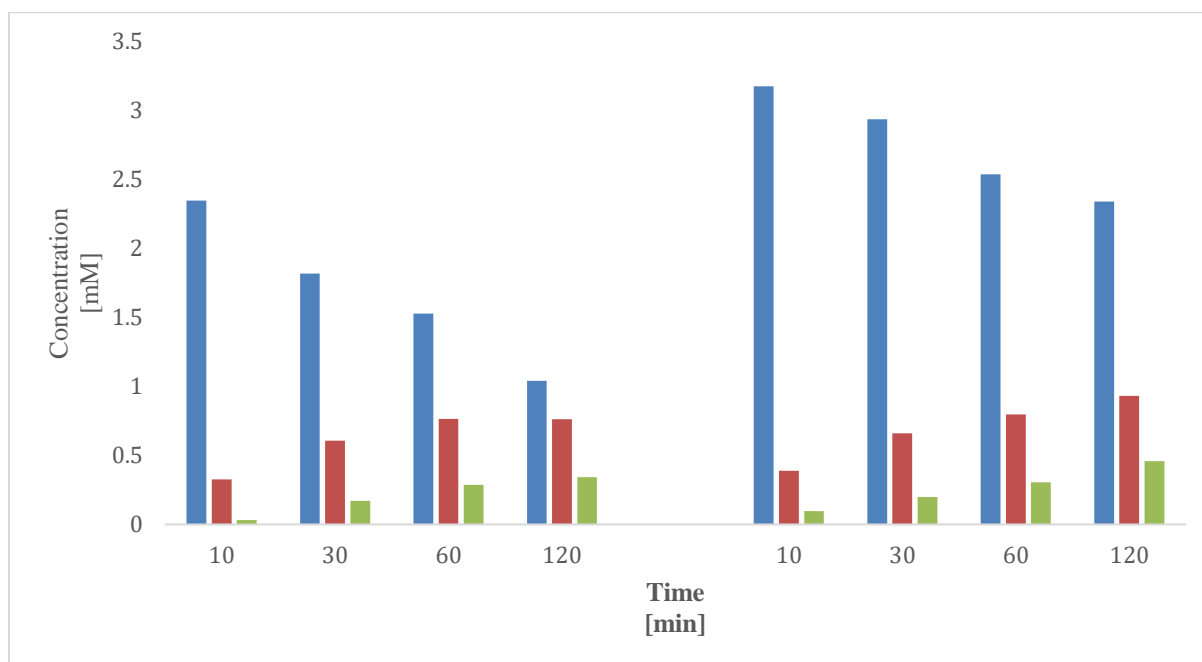


Figure 26. Time courses of aldehyde, alcohol and acid concentrations employing immobilised enzyme during two reaction cycles. Each reaction time was performed over 120 min and was analysed with HPLC. Blue bars show the acid concentration, red bars the aldehyde concentration and green bars the alcohol concentration.

5 Discussion

Gross published a number of studies^{4,5,6,26} about a purified carboxylate reductase from *N. crassa*. In this thesis, *E. coli* was used as host organism for the heterologous expression of a CAR sequence from *N. crassa* NCBI gene accession Nr. CAQ31055.1). According to the lack of information about the protein sequence used in the work of Gross et al. (1968) it could only be assumed that the same protein was investigated. One goal herein was to provide evidence whether the used *NcCAR* sequence (E.C. 1.2.1.30) was identical to the protein described by Gross et al. or not. Furthermore, the knowledge of the *NcCAR* should be extended with this thesis.

The recombinant *NcCAR* was obtained using an autoinduction protocol as mentioned in chapter 3.3 to guarantee correct protein folding.¹ The co-expression of the phosphopantetheinyl transferase was implemented to generate an active CAR, as reviewed by J. Beld.¹⁷ Other published fungal CARs (ATEG03630 (AnCAR), StbB (SbCAR) have been expressed in *S. cerevisiae* or *Aspergillus oryzae*.²⁷ After the expression of the *NcCAR* in *E. coli*, the enzyme was purified as described in 3.4. Compared to the purification procedure by Gross, a distinct difference could be established. Gross et al. (1968) used six purification steps involving protamine and ammonium sulphate precipitation, calcium phosphate gel adsorption, chromatography on TEAE-cellulose and hydroxyapatite, but still the preparation contained minor impurities.⁴ During this thesis, four purification steps were established. During the design of the genetic sequence, an additional six times His-Tag was attached to the N-terminus, to simplify the purification procedure. The first purification contained a gradient of 0 % of buffer-B up to 100 % buffer-B over 10 CVs. Some impurities could be determined in the SDS-PAGE mentioned in chapter 4.1. To improve the purification procedure, a stepwise elution scheme based on imidazole concentrations of 20, 85 and 500 mM in buffer-B, as described in 4.1, was implemented. The corresponding chromatogram showed two elution peaks which were separated and loaded onto an SDS-gel mentioned in 4.2. The resulting SDS-PAGE showed no difference in the protein composition between those two elution peaks, but the stepwise purification improved the purity compared to the gradient purification. Further analysis of the stepwise elution pools delivered no difference in enzyme activity. It was expected that a conformation modification may bring about different enzyme activities, but that was not the case. An explanation may be based on weak bonds between the resin and the *NcCAR*. Finally, the reason for the different elution peaks could not be ascertained. The enzyme characterisation

was performed with both elution pools. Differences in the purity between *NcCAR* and *NiCAR* could occur because of a different folding, resulting in a weak binding to the resin.

As described in chapter 3.4, additional purification steps were performed. The final SDS-PAGE mentioned in 4.1, containing all used processes, like the removal of the His-Tag and an additionally gel filtration, enhanced the purity of the protein. The final gel-filtered protein showed the highest purity. Compared to the purification procedure by Gross, the used protein purification was improved during this Master's thesis.

To ensure a complete activation of the protein, the *NcCAR* activity with additional phosphopantetheinyl was compared to the enzyme activity of *NiCAR* which had not already been activated. The used *NiCAR* passed as a positive control for phosphopantetheinylation, because without additional PPase and CoA the enzyme should be inactive. The results are illustrated in chapter 4.6. It is assumed that the used CAR is close to be completely activated, because an additional encore of phosphopantetheinyl only increased the enzyme activity slightly. It seems, that *NcCAR* showed a relatively higher affinity to the used substrate (hexanoic acid) than *NiCAR*. The dilutions applied decreased the enzyme activity, maybe because of pipette inaccuracy. It is assumed, that the purification and PPTase concentration were sufficient (compare SDS-PAGE in chapter 4.3) to guarantee complete enzyme activation. The different fermentation samples of the PPTase which were separated by SDS-PAGE showed no huge differences for the PPTase while using a heat purification step, compared to the enzyme preparation delivered by Margit Winkler. The final new fermentation of slot 6, which was used for the assay, seemed to have the highest purity and enzyme concentration.

Assuming that the majority of *NcCAR* molecules had been activated *in vivo* by *E. coli*, the substrate scope of *NcCAR* was determined using a spectrophotometric NADPH depletion assay. The substrate list is shown in chapter 4.4. By comparing the results to Gross et al. (1968), the substrates must be related to salicylic acid as reference. The historic enzyme assay was based on the ATP consumption.²⁸

Table 11 Comparison of the enzyme activity results of Gross to the characterized *NcCAR*, estimated with spectrophotometric NADPH depletion assay.

Gross native <i>NcCAR</i>	Recombinant <i>NcCAR</i>
Salicylic acid 100%	Salicylic acid 100%
Benzoic acid 286%	Benzoic acid 392%
3-Hydroxy benzoic acid 150%	3-Hydroxy benzoic acid 178%
4-Hydroxy benzoic acid 150%	4-Hydroxy benzoic acid 142%
Cinnamic acid 229%	Cinnamic acid 446%

By comparing the enzyme activities, a similar trend was observed. Relating the results to salicylic acid, the activity for 3-hydroxy benzoic acid and 4-hydroxy benzoic acid were closely the same. The activity was increased using benzoic acid and cinnamic acid as substrate and was significantly higher by the characterised enzyme compared to the published data. A final, definite conclusion of the accordance of those two enzyme preparations cannot be drawn. The analysed substrates were not the same, as well as the enzyme preparation, fermentation and purification steps. The activities may suggest that the enzyme of this study was already used by Gross. On the other hand, Gross mentioned a limitation on substrates: aliphatic acids showed no enzyme activity under the conditions then. Though, our recombinant *NcCAR* could generate aldehydes from aliphatic acids as shown in Figure 15. Other substrates described by Gross (L-alanine and acetic acid) were not analysed in this thesis. To confirm the production of the corresponding aliphatic aldehydes, direct GC/FID measurements were used and showed indeed aliphatic aldehydes.

The co-solvent tolerance assays led to the conclusion, that a minor negative influence of the used solvents for the enzyme was observed at low co-solvent concentrations. Just higher concentrations - above 4 % of DMSO or methanol - had a distinct impact on the total enzyme activity. The activity of an enzyme under the best pH conditions is important for industrially used enzymes. The pH determination was also done by William Finnigan *et al.*¹⁸ for *mpCAR*, *niCAR*, *noCAR* and *tpCAR*, as well as by Gross⁴ for the native *NcCAR*. The published pH optimum of *N. crassa* CAR was reported between pH 7.7 - 8.1. The determination was based on an endpoint quantification by radiolabelled salicylic aldehyde formation.⁴ The generated spectrophotometric results of chapter 4.7 on the recombinant *NcCAR* accounts for a pH optimum between 5.5 - 6.0 with cinnamic acid as substrate. This result was verified by using a HPLC endpoint measurement of cinnamaldehyde. These diverging results could result from

unequal reaction conditions or additional post-translational modifications of the native *N. crassa* CAR used by Gross et al. (1968). Another possibility might be differences in the amino acid sequences as a result of different strain backgrounds (SY7A versus OR74A)¹. The pH optimum activity of the other mentioned carboxylic acid reductases, analysed by William Finnigan,¹⁸ were determined between pH 7.5 and pH 7.8 with 4-methylbenzoic acid as substrate. This would fit into the published data by Gross. An additional reason for the difference could be the used substrates. Further differences can be found by comparing the optimal temperatures for the enzyme activity. The optimal initial rate activity was observed at 55°C for the recombinant *NcCAR* based on the results of chapter 4.7. This activity was completely lost upon an incubation at these temperatures for 90 min. A reactive enzyme was available just upon an incubation temperature between 35°C and 40°C, and is consistent with a T_m of *NcCAR* of 45.3°C.¹ In the mentioned publication, the *NcCAR* used by Gross for the formation of salicylic acid showed its highest initial activity between 35°C and 36°C. The best temperature conditions for the used enzymes by William Finnigan were different.¹⁸ *TpCAR* was totally inactive after an incubation time of 30 min at 42°C. In contrast, *MpCAR*, a thermostable enzyme from *M. phlei*, retained an activity of 92 % and could retain residual activity up to 50°C. *NiCAR* and *NoCAR* showed intermediate thermostability beyond 44°C. These differences in thermostability could be based on the conformation of the enzymes and on the S-S bonds.¹⁸

Finally, the impact of the pyrophosphate was analysed by HPLC described in chapter 4.11. The influence of the pyrophosphate on the enzymatic reaction was analysed by preparing samples containing pyrophosphatase (PPase) and samples without PPase. By adding PPase to the reaction, the final amount of aldehyde increased from 1.7 to ~ 3 mM. The negative impact of the pyrophosphate, which had already been published,^{19, 20} was confirmed thereby. Furthermore, the kinetic parameters were determined for the purified *NcCAR* using the spectrophotometric assay described in chapter 4.12. The K_M value for cinnamic acid as substrate was 2.317 mM and a V_{max} of 21.08 mM/min was obtained. These data bases are unique for cinnamic acid as substrate and were not found in other sources or literature. For further important substrates, they should be determined again. By summarising all data and comparing them to the published results, it is most likely that recombinant *NcCAR* of this thesis equates to the published native *NcCAR* by Gross in 1968.

Literature

1. Schwendenwein, D., Fiume, G., Weber, H., Rudroff, F. & Winkler, M. Selective Enzymatic Transformation to Aldehydes in vivo by Fungal Carboxylate Reductase from *Neurospora crassa*. *Adv. Synth. Catal.* (2016).
2. Stolterfoht, H., Schwendenwein, D., Sensen, C. W., Rudroff, F. & Winkler, M. Four distinct types of E.C. 1.2.1.30 enzymes can catalyze the reduction of carboxylic acids to aldehydes. *J. Biotechnol.* (2017).
4. Gross, G. G., Bolkart, K. H. & Zenk, M. H. Reduction of cinnamic acid to cinnamaldehyde and alcohol. *Biochem. Biophys. Res. Commun.* 32, (1968).
5. Gross, G. G. & Zenk, M. H. Reduktion aromatischer Säuren zu Aldehyden und Alkoholen im zellfreien System: 2. Reinigung und Eigenschaften von Aryl-Alkohol: NADPH Oxidoreduktase aus *Neurospora crassa*. *Eur. J. Biochem.* 8, (1969).
6. Gross, G. G. Evidence for enzyme-substrate intermediates in the aryl-aldehyde: NADP oxidoreductase catalysed reduction of salicylate 5, (1969).
7. Li, T. & Rosazza, J. P. N. Purification, characterization, and properties of an aryl aldehyde oxidoreductase from *Nocardia* sp. strain NRRL 5646. *J. Bacteriol.* 179, (1997).
8. Scott Hagedorn, Bryan Kaphammer Microbial Biocatalysis in the generation of flavour and fragrance chemicals, *Annu. Rev. Microbial* (1994).
9. Krings, U. & Berger, R. G. Biotechnological production of flavours and fragrances. *Appl. Microbiol. Biotechnol.* 49, (1998).
10. Reuss, G., Disteldorf, W., Gamer, A. O. & Hilt, A. Formaldehyde. *Ullmann's Encycl. Industrial Chem.* 15, (2012).
11. Kunjapur, A. M., Tarasova, Y. & Prather, K. L. J. Synthesis and Accumulation of Aromatic Aldehydes in an Engineered Strain of *Escherichia coli*. *J. Am. Chem. Soc.* 136, (2014).
12. Napora-Wijata, K., Strohmeier, G. A. & Winkler, M. Biocatalytic reduction of carboxylic acids. *Biotechnol. J.* (2014).
13. Akhtar, M. K., Turner, N. J. & Jones, P. R. Carboxylic acid reductase is a versatile enzyme for the conversion of fatty acids into fuels and chemical commodities. *Proc. Natl. Acad. Sci. U. S. A.* 110, (2013).
14. Brown, H. C. & Rao, B. C. S. A new aldehyde synthesis - The reduction of acid chlorides by lithium tri-*t*-butoxyaluminumhydride. *J. Am. Chem. Soc.* 80, (1958).
15. Chandrasekhar, S., Kumar, M. S. & Muralidhar, B. One pot conversion of carboxylic

- acids to aldehydes with DIBAL-H. *Tetrahedron Lett.* 39, 909–910 (1998).
16. Winkler, M. & Winkler, C. K. Trametes versicolor carboxylate reductase uncovered. *Monatshefte für Chemie - Chem. Mon.* 147, 575–578 (2016).
 17. Beld, J., Sonnenschein, E. C., Vickery, C. R., Noel, J. P. & Burkart, M. D. The phosphopantetheinyl transferases: catalysis of a post-translational modification crucial for life. *Nat. Prod. Rep.* 31, (2014).
 18. Finnigan, W. *et al.* Characterization of carboxylic acid reductases as enzymes in the toolbox for synthetic chemistry. (Manuscript in submission). *ChemCatChem* (2016).
 19. Hisanaga, Y. *et al.* Structural basis of the substrate-specific two-step catalysis of long chain fatty acyl-CoA synthetase dimer. *J. Biol. Chem.* 279, (2004).
 20. Kunjapur, A. M. & Prather, K. L. J. Microbial engineering for aldehyde synthesis. *Appl. Environ. Microbiol.* 81, (2015).
 21. Hodgman, C. E. & Jewett, M. C. Cell-free synthetic biology: Thinking outside the cell. *Metab. Eng.* 14, (2012).
 22. Kunjapur, A. M., Cervantes, B. & Prather, K. L. J. Coupling carboxylic acid reductase to inorganic pyrophosphatase enhances cell-free in vitro aldehyde biosynthesis. *Biochem. Eng. J.* 109, (2016).
 23. Chen, Y. & Rosazza, J. P. N. Microbial transformation of ibuprofen by a Nocardia species. *Appl. Environ. Microbiol.* 60, 1292–1296 (1994).
 24. Li, T. & Rosazza, J. P. Biocatalytic synthesis of vanillin. *Appl. Environ. Microbiol.* 66, (2000).
 26. Gross, G. G. Stoichiometric studies on aryl-aldehyde: NADP oxidoreductase from *Neurospora crassa*. *FEBS Lett.* 17, (1971).
 27. Li, C. *et al.* Biosynthesis of LL-Z1272 β : Discovery of a New Member of NRPS-like Enzymes for Aryl-Aldehyde Formation. *ChemBioChem* 17, 904–907 (2016).
 28. Gross, G. G. & Zenk, M. H. Reduktion aromatischer Säuren zu Aldehyden und Alkoholen im zellfreien System. *Eur. J. Biochem.* 8, (1969).
 29. Margit Winkler, Katharina Dokulil, The Nitrile forming Enzyme 7-Cyano-7-deazaguanine Synthase from *Geobacillus kaustophilus*: A reverse Nitrilase *ChemBioChem* 2373 - 2378 (2015)

6 Appendix

6.1.1 Centrifuges and associated materials

Centrifuge 5810 R, Eppendorf AG, Hamburg, Germany

Centrifuge 5415 R, Eppendorf AG, Hamburg, Germany

Avanti™ centrifuge J-20 XP/Beckman Coulter™, Inc, Vienna, Austria

Nalgene® Labware 500 ml PPCO Centrifuge Bottles, Thermo Scientific, Rochester, NY, USA

Ultracentrifuge Optima LE80K/Beckman Coulter™, Inc Vienna, Austria

6.1.2 Fast protein liquid chromatography (FPLC) and materials

ÄKTA Purifier 100 with Frac-950, GE Healthcare Europe GmbH, Vienna, Austria

ÄKTA Prime, GE Healthcare Europe GmbH, Vienna, Austria

HiLoad™ 16/60 Superdex™ 200 prep grade 120 ml, GE Healthcare, Europe GmbH, Vienna, Austria

HiPrep™ 26/10 Desalting, GE Healthcare Europe GmbH, Vienna, Austria

HiTrap™ FF, 5 ml, GE Healthcare Europe GmbH, Vienna, Austria

Sample pump P-950, GE Healthcare Europe GmbH, Vienna, Austria

Cellulose acetate filter, 0.2 µl pore size, Sartorius Mechatronics Austria GmbH, Vienna, Austria

6.1.3 SDS-PAGE and materials

PowerEase 500 power supply: Invitrogen™ life technologies, Lofer, Austria

Bolt® 4-12% Bis-Tris Plus Gels, 10-well Life technologies, Vienna, Austria

Bolt® 4-12% Bis-Tris Plus Gels, 15-well Life technologies, Vienna, Austria

Bolt MOPS SDS running buffer

Ladder

SimplyBlue™ Safe-Stain solution

6.1.4 HPLC and associated materials

HPLC-UV Agilent 1100 series

G1316A thermostated column compartment (TCC)

G1321B fluorescence detector (1260 FLD)

G1379A degasser

G3111A quaternary pump

G1367A high performance autosampler WPLAS

G1330B ASL thermostat

G1316A thermostated column compartment

G1315B diode array detector

G1364C fraction collector

6.1.4.1 HPLC-MS Agilent 1200 series

G1379B degasser

G1312B binary pump SL

G1367C high performance autosampler SL

G1310A isocratic pump

G1314 variable wavelength detector SL

6120 Agilent Technologies, quadrupole LC/MS detector with a G1918B electrospray ionization source

G1316B thermostatic column compartment

6.1.5 GC-FID

Agilent Technologies 6890N Network GC system

6.1.6 Columns

Chromolith performance RP 18E 4.6x100 mm HPLC Column for HPLC

Phenomenex Gemin[®] NX 3 C18 110 Å, LC column (150 x 2.0 mm) with a SecurityGuard[™] Cartridge 4 x2.0 mm column

HiTrap[™] FF 5 ml columns for ÄKTA

Varian cp 7503 CP chirasil DEX CB column (25 m x 320 µm x 0.25 µm) for GC

Phenomenex Kinetex Biphenyl, 3 µ; 110 Å; 2 x 150 mm column

6.1.7 Photometer and associated materials

Nanodrop 2000c Spectrophotometer, PEQLAB Biotechnologie, Germany

BioPhotometer Plus, Eppendorf AG, Hamburg, Germany

Synergy Mx Platereader, BioTek, USA

Cuvettes (10 x 4 x 45 mm), Sarstedt, Germany

6.1.8 Reaction vessels

Micro-centrifuge tubes, 1.5 ml with lid, Greiner Bio GmbH, Frickenhausen, Germany

50 ml Greiner tube, Greiner Bio GmbH, Frickenhausen, Germany

15 ml Greiner tube, Greiner Bio GmbH Frickenhausen, Germany

300 ml shaking flasks with baffles

2 l Shaking flasks with baffles

6.1.9 Shakers and incubators

Titramax 1000, Heidolph Instruments, Schwabach, Germany

RS 306 rotary shaker (50 mm), Infors AG, Bottmingen-Basel, Switzerland

Thermomixer comfort (1.5 ml), Eppendorf AG, Hamburg, Germany

Multitron II incubator shaker, Infors AG, Bottmingen-Basel, Switzerland

Binder drying oven, Binder GmbH Tuttlingen, Germany

6.1.10 Additional instruments and materials

Vortex-Genie 2, Scientific Industries Inc., Bohemia, NY, USA

Vivaspin 20 centrifugal concentrators, 30.000 MWCO PES, Sartorius AG, Göttingen, Germany

ABS 220-4 analytical balance, Kern & Sohn GmbH, Balingen, Germany

GP3202 Precision Balance, Sartorius AG, Göttingen, Germany

6.2 Reagents, buffers, stocks and media

Table 12. Detailed buffer composition

Name	Reagents	Elemental formula	Concentration
20xNPS	Ammonium sulphate	(NH ₄) ₂ SO ₄	0.5 mol/l
	Monopotassium dihydrogen phosphate	KH ₂ PO ₄	1 mol/l
	Disodium hydrogen phosphate	Na ₂ HPO ₄	1 mol/l
50x5052	Glycerol	C ₃ H ₈ O ₃	2.7 mol/l
	Glucose	C ₆ H ₁₂ O ₆	0.14 mol/l
	α-Lactose	C ₁₂ H ₂₂ O ₁₂	0.29 mol/l
40% Glucose	Glucose in ddH ₂ O	C ₆ H ₁₂ O ₆	2.22 mol/l
1 M MgSO ₄	Magnesium sulphate	MgSO ₄	1 mol/l
10 % Agarose Gel	Agar	C ₁₂ H ₁₈ O ₉	1 g/l
Ampicillin	Ampicillin, in ddH ₂ O	C ₁₆ H ₁₉ N ₃ O ₄ S	50 mg/ml

Buffer A pH 7.4 adjusted with HCl	Imidazole	$C_3H_4N_2$	10 mM
	Sodium chloride	NaCl	500 mM
	Potassium dihydrogen phosphate	KH_2PO_4	20 mM
Buffer B pH 7.4 adjusted with HCl	Imidazole	$C_3H_4N_2$	500 mM
	Sodium chloride	NaCl	500 mM
	Potassium dihydrogen phosphate	KH_2PO_4	20 mM
CAR-Storage Buffer pH 7.5 adjusted with KOH	2-(N-morpholino) ethane sulfonic acid (MES)	$C_6H_{13}NO_4S$	50 mM
	Magnesium chloride	MgCl	10 mM
	Ethylenediaminetetraacetic acid (EDTA)	$C_{10}H_{16}N_2O_8$	1 mM
	Dithiothreitol (DTT)	$C_4H_{10}O_2S_2$	1 mM
HPLC eluent A	Ammonium acetate	$C_2H_3O_2NH_4$	5 mM
	Acetic acid	CH ₃ COOH	83 mM
HPLC eluent B	Acetonitrile	C_2H_3N	100 %

6.3 Received organisms

pET-Duet1_*Ec*PPTaseHTNcCAR vector in *E. coli* (Margit Winkler)

pEHISTEV_NiCAR_opt vector in *E. coli BL21 Gold* (Margit Winkler)

6.4 Software

Sigmaplot 13.0, GSL Biotech LLC, USA

SnapGene® Viewer, Version 3.1.1

Unicorn™ 6.3, GE Healthcare Europe GmbH, Vienna, Austria

Software PrimeView 5.0, Life Scinces, GE Healthcare Europe GmbH, Vienna, Austria

Software ©Rob Beynon